

Aus der Medizinischen Klinik mit Schwerpunkt Nephrologie und
internistische Intensivmedizin der Medizinischen Fakultät
Charité – Universitätsmedizin Berlin

DISSERTATION

Schlaganfall abhängige Mechanismen der endothelialen
autoimmunen PAR2 Aktivierung
Stroke dependent mechanisms of endothelial autoimmune PAR2
activation

zur Erlangung des akademischen Grades
Doctor medicinae (Dr. med.)

vorgelegt der Medizinischen Fakultät
Charité – Universitätsmedizin Berlin

von

Hongfan Zhao
aus Henan, China

Datum der Promotion: 03.03.2023

Table of Contents

Abbreviations	4
List of Tables	7
List of Figures	8
Abstract	10
Abstrakt	12
1. Introduction	14
1.1 Clinical background	14
1.2 Angiogenesis	14
1.3 VEGF as the main regulator of angiogenesis	15
1.3.1 VEGF	15
1.3.2 VEGF in health and different diseases	15
1.3.3 Regulation of VEGF	16
1.4 Protease-activated receptor 2 (PAR2)	17
1.4.1 Protease-activated receptor family (PAR)	17
1.4.2 PAR2	18
1.4.3 PAR2 activating mechanism	19
1.4.4 PAR2 intracellular signaling pathways	19
1.4.5 Physiological and pathological roles of PAR2	21
1.5 Autoantibodies targeting GPCR	22
1.5.1 Autoantibodies targeting GPCR in human pathology	22
1.5.2 Autoantibodies against PAR2	23
2. Hypothesis and Objectives	23
2.1 Hypothesis	23
2.2 Objectives	24
3. Materials and Methods	25
3.1 Materials	25
3.1.1 Chemical substances	25
3.1.2 Equipment	28

3.1.3 Kits	29
3.1.4 Plasmid, bacteria, cell lines and enzymes	30
3.1.5 Antibodies	31
3.1.6 Buffer recipes	31
3.1.7 Media	33
3.1.8 Primers	35
3.2 Methods	36
3.2.1 RNA extraction, cDNA production and qRT-PCR	36
3.2.2 Generation of PAR2-HiBiT constructs	38
3.2.3 Patient IgG isolation	40
3.2.4 Cell culture and stimulation	41
3.2.5 Matrigel angiogenesis assay	42
3.2.6 Luciferase reporter assay	42
3.2.7 Nano-GLO [®] HiBiT Extracellular Detection assay	43
3.2.8 Dual luciferase reporter assay	43
3.2.9 Western blot	43
3.2.10 ELISA	44
3.2.11 Statistical analysis	44
4. Results	45
4.1 Trypsin- and PAR2-IgG-induced angiogenesis in HMEC-1	45
4.1.1 Trypsin and Q1-3 PAR2-IgG increased angiogenesis in HMEC-1	45
4.1.2 Angiogenic genes involved in trypsin-induced tube formation	46
4.2 PAR2 induced G-protein activation and intracellular ERK1/2 signaling	49
4.2.1 G-protein activation of PAR2 by Q1-3 and Q4 PAR2-IgG	49
4.2.2 Trypsin time- and dose-dependently induced endothelial ERK1/2 and Akt signaling	51
4.2.3 Q1-3 PAR2-IgG induced stronger endothelial ERK1/2 and Akt signaling	52
4.2.4 Function of PAR2 extracellular loops in G-protein activation in HMEC-1	53

4.2.5 Trypsin and PAR2-IgG induced PAR2 internalization in HMEC-1	57
4.3 Role of PAR2 in PAR2-IgG-induced G-protein and ERK1/2 activations	58
4.3.1 PAR2 mediates Q1-3 PAR2-IgG-induced $G_{q/11}$ and ERK1/2 activations	59
4.3.2 Trypsin-induced expression of angiogenic genes and released respective proteins is ERK1/2 dependent	59
4.3.3 Involvement of PAR2 and ERK1/2 signaling in the regulation of angiogenic genes and protein releases by PAR2-IgG	62
4.4 Regulatory mechanism of trypsin and PAR2-IgG-induced VEGF transcription	65
4.4.1 Detection of transcription factor binding sites regulating VEGF promoter activity induced by trypsin and PAR2-IgG	65
4.4.2 Involvement of AP-1 in <i>VEGF</i> promoter activation in HMEC-1	66
4.5 PAR2/ERK1/2 signaling were involved in PAR2-IgG-induced endothelial angiogenesis	67
4.6 Effect of PAR2-IgG on angiogenesis in brain microvascular endothelial cells	68
5. Discussion	70
5.1 Characteristics of PAR2-IgG isolated from stroke patients	70
5.2 G-protein coupling of PAR2	72
5.3 PAR2 and VEGF/VEGFR signaling	73
5.4 PAR2 and angiogenesis signaling	74
5.5 ECLs and PAR2 activation	75
6. Future Prospects	76
References	78
Statutory Declaration	87
Curriculum Vitae	88
Publications	89
Acknowledgements	90
Confirmation by a statistician	91

Abbreviations

AC	Adenylyl cyclase
AIS	Acute ischemic stroke
ANG2	Angiopoietin 2
AP-1	Activating protein-1
AT ₁ R	Angiotensin II type 1 receptor
B2M	Beta-2 microglobulin
bp	Base pair
cAMP	Cyclic adenosine monophosphate
cDNA	Complementary DNA
Conc	Concentration
CREB	Cyclic AMP (cAMP)-response element-binding protein 1
CXCL1	Chemokine (C-X-C motif) ligand 1
DAG	Diacylglycerol
DMEM	Dulbecco's modified Eagle medium
DMSO	Dimethyl sulfoxide
EAA	Endothelial autoantibodies
EC	Endothelial cells
ECL	Extracellular loop
EGF	Epidermal growth factor
ERK1/2	Extracellular signal-regulated kinases 1 and 2
ERKB	ERK blocker
ET _A R	Endothelin-1 type A receptor
EVT	Endovascular treatment
F2RL1	Coagulation factor II receptor-like 1
FCS	Fetal calf serum
Foxo6	Forkhead box protein O6

GAPDH	Glyceraldehyde 3-phosphate dehydrogenase
GPCR	G-protein-coupled receptor
GRK	G-protein-coupled receptor kinase
hCMEC/D3	Human cerebral microvascular endothelial cells
HIF-1	Hypoxia inducible factor 1
HMEC-1	Human microvascular endothelial cells
ICLs	Intracellular loops
IgG	Immunoglobulin class G
IL-6	Interleukin 6
IL-8	Interleukin 8
IP3	Inositol triphosphate
IV-rtPA	Intravenous recombinant tissue plasminogen activator
JNK	c-Jun kinase
Kb	Kilobase
kD	Kilodalton
LB	Lysogeny broth
MAPK	Mitogen-activated protein kinase
mM	Millimolar
NFAT	Nuclear factor of activated T-cells
NF- κ B	Nuclear Factor κ B
ng	Nanogram
PAR1	Protease-activated receptor 1
PAR2	Protease-activated receptor 2
PAR2-AP	PAR2-activating peptide
PAR2B	PAR2 peptide blocker
PAR3	Protease-activated receptor 3
PAR4	Protease-activated receptor 4

PAR	Protease-activated receptor
PBS	Dulbecco's phosphate buffered saline
PCR	Polymerase chain reaction
PKA	Protein kinase A
PKC	Protein kinase C
PLC	Phospholipase C
qRT-PCR	Quantitative real-time PCR
RA	Rheumatoid arthritis
RhoA	Ras homologue A
RhoGEF	Ras homologue guanine nucleotide-exchange factor
RNA	Ribonucleic acid
SEM	Standard error of the mean
Sp1	Specificity protein 1
SRF	Serum response factor
SS	Sjögren's syndrome
STAT3	Signal transducer and activator of transcription 3
TGF	Tumor growth factor
Tie2	TEK receptor tyrosine kinase
TMs	Transmembrane domains
TSH	Thyrotropin, thyroid stimulating hormone
TSHR	Thyroid stimulating hormone receptor
VEGF	Vascular endothelial growth factor
VEGF-R	Vascular endothelial growth factor receptor
α 1AR	α 1-adrenergic receptor
β 1AR	β 1-adrenergic receptor
μ g	Microgram
μ L	Microliter

List of Tables

Table 1. Primers for mutant generation	35
Table 2. Primers for sequencing	35
Table 3. Primers for quantitative real-time PCR	36
Table 4. cDNA synthesis components	37
Table 5. RT-PCR reaction conditions	37
Table 6. qRT-PCR program	38
Table 7. qRT-PCR components	38
Table 8. Mutagenesis reaction components	39
Table 9. Mutagenesis PCR reaction conditions	39
Table 10. KLD reaction system	39
Table 11. Initial number of cells in different cell culture vessels	41

List of Figures

Figure 1. Cleavage and activation process of PARs.....	18
Figure 2. Classical downstream signaling pathways of PAR2.....	20
Figure 3. Effects of trypsin and PAR2-IgG on endothelial cell tube formation.....	46
Figure 4. Time-dependent increase of endothelial angiogenic gene expressions in response to trypsin.....	47
Figure 5. Trypsin increased dose-dependent angiogenic genes transcription.....	48
Figure 6. Trypsin increased dose-dependent angiogenic cytokine release.....	49
Figure 7. Schematic overview of major GPCR signaling pathways and relevant response elements.....	50
Figure 8. Effects of PAR2-IgG on $G_{q/11}$ or $G_{\alpha 12/13}$ and ERK1/2 activation.....	51
Figure 9. Time- and dose-dependent trypsin-induced endothelial ERK1/2 and Akt activation.....	52
Figure 10. Q1-3 PAR2-IgG induced stronger endothelial ERK1/2 and Akt activation via PAR2.....	53
Figure 11. Q1-3 PAR2-IgG-activated $G_{q/11}$ in wild-type or mutated ECLs of PAR2-expressing HMEC-1.....	54
Figure 12. Q4 PAR2-IgG-activated $G_{q/11}$ in wild-type or mutated ECLs of PAR2-expressing HMEC-1.....	55
Figure 13. Q1-3 PAR2-IgG-activated ERK1/2 in wild-type or mutated ECLs of PAR2-expressing HMEC-1.....	56
Figure 14. Q4 PAR2-IgG-activated ERK1/2 in wild-type or mutated ECLs of	

PAR2-expressing HMEC-1	57
Figure 15. PAR2 expression at the plasma membrane	58
Figure 16. PAR2 inhibition reduced $G_{q/11}$ and ERK1/2 activation by PAR2-IgG in HMEC-1	59
Figure 17. Trypsin-induced expression of angiogenic genes is ERK1/2-dependent. .	60
Figure 18. Trypsin-induced release of angiogenic cytokines is ERK1/2-dependent. .	61
Figure 19. PAR2- and ERK1/2-dependence of PAR2-IgG induced expressions of endothelial angiogenic genes.	63
Figure 20. PAR2-IgG induces endothelial angiogenic cytokine release via PAR2 and ERK1/2 signaling.	64
Figure 21. Detection of transcription factor binding sites regulating VEGF promoter activity induced by trypsin and PAR2-IgG.	66
Figure 22. Effect of AP-1 inhibitor on human <i>VEGF</i> promoter in response to trypsin and PAR2-IgG.	67
Figure 23. PAR2-IgG regulated endothelial cell tube formation via PAR2/ERK1/2 signaling pathway.	68
Figure 24. Effect of PAR2-IgG on hCMEC/D3 tube formation.	69

Abstract

Background:

Protease-activated receptor 2 (PAR2) is broadly expressed on endothelial cells contributing to inflammatory processes and angiogenesis. Autoantibodies against PAR2 can regulate these functions in health and disease. Recently, a collaboration group discovered in a prospective observational cohort study that stroke patients with a higher concentration (highest quartile Q4) of PAR2-IgG presented a poor clinical outcome compared to others (lower quartiles Q1-3). However, the biological functions and molecular mechanism remain unclear. Therefore this study aims to explore the possible function of PAR2-IgG on endothelial-based angiogenesis which might have an essential impact on clinical outcome after stroke.

Methods:

IgGs were isolated from the sera of stroke patients (Q1-3 and Q4), then Matrigel angiogenesis assay was used to study vascular tube formation by IgGs and the natural PAR2 agonist trypsin in vascular endothelial cells (HMEC-1 and hCMEC/D3, a blood-brain barrier human endothelial cell line). Additionally, qRT-PCR, western blot, and ELISA were used to investigate the angiogenic signaling pathways. The activation of G-protein subunits was examined by the Luciferase reporter assay, based on mutations of wild-type PAR2 and extracellular loops (ECLs). The receptor internalization was studied by Nano-Glo[®]HiBiT detection assay. The main inductor of angiogenesis VEGF was examined in detail by promoter assay with regard to the activation of the promoter and potential binding fragments of transcription factors.

Results:

The PAR2 agonist trypsin was involved in the regulation of mRNA synthesis and protein release of VEGF, IL-6, IL-8, CXCL1 and ANG2 through the ERK1/2 signaling pathway, which promoted vascular tube formation of HMEC-1. Q1-3 PAR2-IgG enhanced angiogenesis via PAR2-ERK1/2-induced angiogenic cytokines and receptor internalization when compared to Q4 PAR2-IgG. Q1-3 PAR2-IgG

triggered $G_{q/11}$ activation -, but not $G_{12/13}$ -, and the mutation of ECL1-3 did not alter the activation. As for Q4, the ECL3 mutation increased the $G_{q/11}$ activation and ERK1/2 activation. Different truncations of the VEGF promoter assay confirmed the binding sites of transcription factors located in the *VEGF* promoter sequence -1339 to -839 bp, and the inhibition of AP-1 completely blocked the promoter activation. To summarize, in contrast to the Q4 group, Q1-3 PAR2-IgG induced greater receptor internalization, $G_{q/11}$ activation, ERK1/2 activation, and angiogenic gene production, which resulted in increased formation of vascular tubes.

Conclusion:

The present work elucidated new PAR2 signaling pathways that are induced by PAR2-IgG in human endothelial cells and identified contrary functional consequences on the angiogenesis of PAR2-IgGs from two different stroke patient cohorts classified by different PAR2-IgG titer ranges. Novel therapeutics modulating PAR2-IgGs in stroke patients might thereby already limit stroke progression at an early stage and lead to improved clinical outcome.

Abstrakt

Hintergrund:

Protease-aktivierter Rezeptor 2 (PAR2) ist auf Endothelzellen hoch exprimiert und reguliert inflammatorische Prozesse und Angiogenese. Autoantikörper gegen PAR2 können diese Funktionen physiologisch und pathophysiologisch beeinflussen. Vor kurzem entdeckten Kollaborationspartner in einer prospektiven Kohortenstudie, dass Schlaganfallpatienten mit hohen PAR2-Spiegeln (höchstes Quartil Q4) einen schlechteren klinischen Outcome hatten als Patienten mit niedrigeren Spiegeln (Quartile Q1-3). Die molekularen Mechanismen dafür waren allerdings ungeklärt. Es war daher das Ziel dieser Studie, eine mögliche Bedeutung dieser PAR2-IgGs auf endotheliale Angiogenese zu untersuchen, die sich positiv auf den klinischen Outcome auswirken könnten.

Methoden:

IgGs wurden von Schlaganfallpatienten (Q1-3 und Q4) isoliert und dann der Matrigel Angiogenese Assay benutzt, um Gefäßbildungen von Endothelzellen (HMEC-1 und hCMEC/D3, einer humanen Bluthirnschranken-Endothelzelllinie) durch die IgGs und den natürlichen Agonisten von PAR2, Trypsin, zu untersuchen. Weiterhin dienten qRT-PCR, Westernblots und ELISA zur Erforschung angiogenetischer Signalwege. Luziferase-Reporter-Assays wurden durchgeführt, um die Aktivierung von G-Protein-Untereinheiten mithilfe von Mutationen von Wildtyp-PAR2 und der extrazellulären Schleifen (ECLs) zu untersuchen. Die Internalisierung des Rezeptors wurde visualisiert mit dem Nano-Glo® HiBiT Detektionsassay. Der Hauptaktivator der Angiogenese, VEGF, wurde detailliert untersucht mithilfe von Promotoraktivierungsstudien und Bindungsfragmente.

Ergebnisse:

Der PAR2 Agonist Trypsin beeinflusste die mRNA Synthese und Proteinfreisetzung von VEGF, IL-6, IL-8, CXCL1 und ANG2 über den ERK1/2 Signalweg und förderte die Ausbildung vaskulärer Gefäßschläuche in HMEC-1. Im Vergleich zu Q4 PAR2-IgG erhöhte Q1-3 PAR2-IgG Angiogenese durch Freisetzung von

angiogentischer Zytokine über PAR2-ERK1/2-Aktivierung und Rezeptorinternalisierung. Q1-3 PAR2-IgG triggerte die Aktivierung von $G_{q/11}$, aber nicht von $G_{12/13}$, und Mutationen von ECL1-3 hatten keinen Einfluss auf die Aktivierung. VEGF Promotorassays bestätigten die Bindungsstelle des Transkriptionsfaktors AP-1 an der *VEGF*-Promotorsequenz -1339 bis -839 bp. Zusammenfassend induzierte Q1-3 PAR2-IgG im Gegensatz zu Q4 PAR2-IgG eine verstärkte Rezeptorinternalisierung, $G_{q/11}$ – und ERK1/2-Aktivierung und Induktion angiogenetischer Gene, was in einer verstärkten Netzwerkbildung resultierte.

Schlussfolgerung:

Die hier dargestellte Arbeit beschreibt neue Signalwege von PAR2 in humanen Endothelzellen, die durch PAR2-IgG aktiviert werden und identifizierte gegensätzliche Auswirkungen auf Angiogenese durch PAR2-IgG von zwei unterschiedlichen Schlaganfallkohorten mit besonders hohen (Q4) oder niedrig-mäßigen (Q1-3) PAR2-IgG-Spiegeln. Die Modulation von PAR2-IgGs könnte eine neue Therapieform bei Schlaganfall darstellen, um die Progression im Verlauf zu verhindern und zu verbessertem klinischem Outcome zu führen.

1. Introduction

1.1 Clinical background

Stroke is one of the leading causes of mortality and of disability globally [1]. Acute ischemic stroke (AIS) emanates from the sudden blockade of an arterial supply to parts of the brain [2]. Thrombolysis is currently the preferred treatment option for AIS. Pharmacological (intravenous recombinant tissue plasminogen activator, IV-rtPA) or mechanical (endovascular treatment, EVT) interventions can recanalize the occlusion and reperfuse the brain tissues [3]. Although therapies for AIS have improved significantly, more than 50% of patients do not recover completely or die [4]. Post-stroke, cerebral endothelium dysfunction takes center stage in injury and repair by promoting oxidative stress, release of angiogenic and inflammatory factors, and regulating blood-brain barrier function [5]. Notably, a lot of evidence points to enhancement of microvessel density as one of the therapeutic strategies to promote functional recovery after ischemic stroke [6-8] and angiogenesis has been suggested to be the target for post-stroke recovery [9]. Hence, the focus of this work lies on endothelium-based angiogenesis.

1.2 Angiogenesis

Angiogenesis refers to the formation of new blood vessels based on the pre-existing vessels, which results from the association of endothelial cells into stable tubes in a complex process of endothelial cell differentiation, proliferation, migration, and rearrangement [10]. Under conditions of vascular injury, hypoxia and inflammation, the production or release of pro-angiogenic factors or inflammatory factors can activate angiogenic signals of quiescent endothelial cells to promote vascular repair and recovery [11]. Angiogenesis is involved in human physiology such as embryonic development and wound-healing, but is also critical in several diseases such as

ischemic stroke, tumor growth, and retinopathies [12]. Following ischemic stroke, it has been shown that angiogenesis occurs in the peri-infarct regions with beneficial impacts on the recovery of blood flow, neuronal metabolism and survival of patients as well as animals [13, 14]. Endothelium, as an inner lining of blood vessels, can respond to various angiogenic factors which are responsible for the angiogenesis regulation [15]. Vascular endothelial growth factor (VEGF), as a major player in angiogenesis, has been verified in multiple relevant researches [16]. There are also several other factors such as Interleukin 6 (IL-6), Chemokine (C-X-C motif) ligand 1 (CXCL1), and Interleukin 8 (IL-8) taking pro-angiogenic effects [17-19]. In addition, Angiopoietin 2 (ANG2), as an antagonist of Angiopoietin 1 (Ang1), has been reported to lead to endothelial destabilization, increased vascular permeability, and pathological angiogenesis via inactivation of TEK receptor tyrosine kinase (Tie2) downstream signals [20].

1.3 VEGF as the main regulator of angiogenesis

1.3.1 VEGF

VEGF was isolated over 30 years ago [21]. The VEGF family is composed of five members, namely: VEGFA, VEGFB, VEGFC, VEGFD, placental growth factor (PLGF). VEGFA, generally named VEGF, is the main regulator of angiogenesis in vascular homeostasis and pathologies [22]. Human VEGFA is located on chromosome 6p12 and has 8 exons [23]. There are five major isoforms of VEGFA including VEGF121, VEGF145, VEGF165, VEGF189, and VEGF206 due to mRNA alternative splicing and proteolytic processing. VEGF165 is the most important isoform of VEGFA [24].

1.3.2 VEGF in health and different diseases

The primary role of VEGF in angiogenesis is appreciated in several physiological and pathological settings [22].

Angiogenesis via VEGF participates in physiological conditions such as pregnancy, embryonic development, endochondral bone formation, skeletal growth, and endocrine gland development [16, 25-27]. Cerebral angiogenesis via VEGF also contributes to neurogenesis [28].

Dysregulation of the VEGF pathway is implicated in several vasculopathies including ischemic stroke and general brain injuries. Cerebral angiogenesis via VEGF is therefore a pathophysiological target in post-ischemic vascular repair, neuroprotection, and post-ischemic brain injury [28]. Interestingly, multiple *in vivo* experimental studies have demonstrated that VEGF is beneficial to ischemic stroke outcome [29-31]. Intraventricular injection of VEGF produces endothelial angiogenesis and neuronal protective effects by lessening infarct size and brain edema formation in mice models with ischemic stroke [29, 30]. Moreover, single intracerebroventricular infusion of VEGF protects the brain against ischemic stroke without increasing blood-brain barrier permeability [31]. Furthermore, VEGF involves a variety of diseases such as inflammatory disorders, cancers, and intraocular neovascular syndromes [16].

1.3.3 Regulation of VEGF

In physiological processes, the levels of VEGF are tightly controlled by rate limiting and potentially negative feedback mechanisms. Insufficient or excess levels of VEGF occur in several pathological processes, such as hypoxic conditions, endocrine diseases, inflammation, and tumorigenesis [16]. Hypoxia, for instance, enhances the transcriptional activity and protein level of hypoxia-inducible factor 1 (HIF-1), which

can up-regulate VEGF via binding to the hypoxia response element of *VEGF* [32]. Growth factors including epidermal growth factor (EGF) and tumor growth factor (TGF), and inflammatory cytokines including IL-1 α and IL-6 can promote the secretion of VEGF [16, 33]. Mutation of (Rat sarcoma virus) Ras oncogene, or PTEN tumor suppressor gene can up-regulate VEGF through the genes Wingless and Int-1(Wnt) and/or the phosphoinositide 3 kinase (PI3K)/Protein kinase B (Akt) pathways [34, 35]. In addition, accumulated evidence has confirmed that down-regulated activity of extracellular signal-regulated kinase 1/2 (ERK1/2) results in a significant reduction in VEGF secretion by myeloma cells, and that hyperbaric oxygen promotes gene transcription of *VEGF* through the ERK1/2-activating protein-1 (AP-1) pathway [36, 37]. Activation of protease-activated receptor 2 (PAR2) on the membrane of glioblastoma cell lines can produce VEGF through the ERK1/2 pathways [38].

1.4 Protease-activated receptor 2 (PAR2)

1.4.1 Protease-activated receptor family (PAR)

PARs are members of the G-protein-coupled receptors (GPCR) family that are switched on by serine proteases. These proteases activate the receptors by cleaving them at the N-terminal domain. After cleavage, the exposed tethered ligand binds intra-molecularly to activate downstream signals with resultant functional significance (Figure.1) [39].

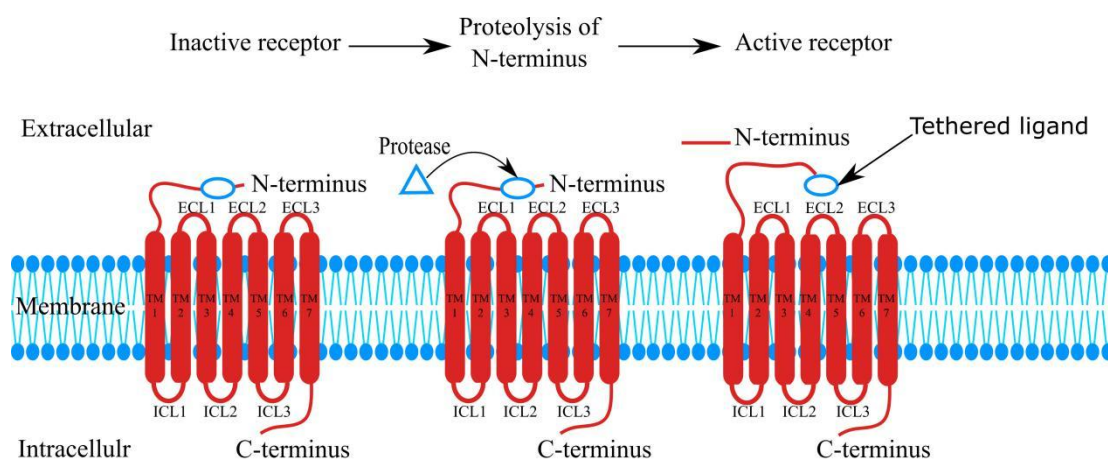


Figure 1. Cleavage and activation process of PARs. (This figure is drawn by the author using Inkscape software). ECL, extracellular loop; TM, transmembrane domain; ICL, intracellular loop.

Protease-activated receptors are classified based on specific ligand characterization. The predominant subtype, PAR1, which is activated by thrombin, trypsin and other serine proteases, was first discovered thirty years ago [40]. Subsequently, three other sub-types, i.e., PAR2, PAR3 and PAR4, were identified through complementary DNA screening. It is known that thrombin can cleave all the subtypes of PAR except PAR2 [40]. PARs are implicated in a plethora of pathophysiological processes, such as vasculopathies, inflammation and tumorigenesis [41]. Therapeutic antibodies and allosteric modulators have been developed to neutralize or inhibit pathological effects of PARs [42, 43].

1.4.2 PAR2

PAR2, also named coagulation factor II receptor-like 1 (F2RL1), G-protein-coupled receptor 11, and PAR1 (FR2) like trypsin receptor 1, was the second member discovered in the PAR family [44]. The encoded gene of human PAR2 locates on chromosome 5q13. The PAR2 protein, constituted of 687 amino acids, is predicted to weigh about 44 kD [45]. PAR2 is abundantly expressed in various tissues including vasculature, brain, skin, lung, colon, uterus and prostate as well as in epithelial cells,

vascular endothelial cells (EC), fibroblasts, neuronal cells and keratinocytes [46]. The principal natural agonists of PAR2 are trypsin, tryptase, and factor Xa/VIIa [44].

1.4.3 PAR2 activating mechanism

PAR2 is a typical GPCR with an extracellular N-terminus domain, three extracellular loops (ECLs), seven transmembrane domains (TMs), three intracellular loops (ICLs), and an intracellular C terminus (Figure.1). Canonically, irreversible cleavage at the enzymatic site SKGR³⁶↓S³⁷LIGKV of the N-terminus by trypsin or another protease can generate a new N-terminus, which binds to extracellular loops (ECLs), especially ECL2 as a tethered ligand [44, 47]. Upon activation by the new ligand, the C-terminus of the receptor binds to a partner G-protein and promotes a transformation from guanosine triphosphate (GTP) to diphosphate (GDP), triggering the dissociation of the G_α from G_{βγ} subunits, initiating downstream signaling [48]. The TM regions of PAR2 have also been identified as interacting with synthetic agonists (GB110) and antagonists (GB88) [49]. Non-canonical agonists including neutrophil elastase, cathepsin G and proteinase-3 also interact at distinct sites of PAR2 to produce biased G-protein subunits activation [50]. Biased signaling could provide a tough task in comprehending the signaling mechanisms of biological receptors and the development of therapeutic agents. Studies have also demonstrated that biased signaling profiles such as Ca²⁺ and mitogen-activated protein kinase (MAPK) are specific to the type of ligand, as well as the cell type expressing the receptor and the assays used in monitoring the G-protein activation [51-54].

1.4.4 PAR2 intracellular signaling pathways

Ligand activation of PAR2 sets off a network of signaling mechanisms involving cognate G-protein subtypes like G_{q/11}, G_{α12/13}, G_{αs}, G_i or G_{βγ} (Figure.2) [55, 56].

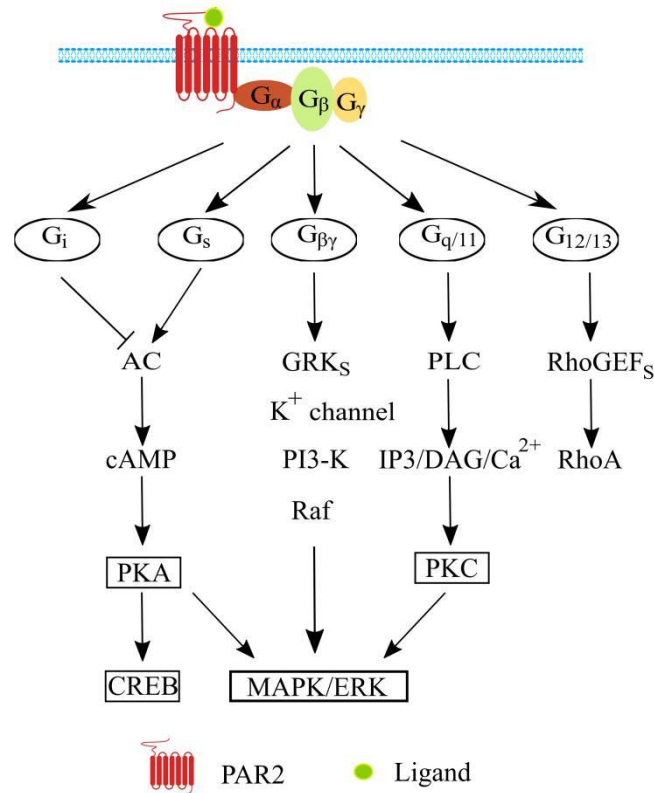


Figure 2. Classical downstream signaling pathways of PAR2. (This figure is drawn by the author using Inkscape software). AC, Adenylyl cyclase; cAMP, Cyclic adenosine 3',5'-monophosphate; PKA, protein kinase A; PKC, protein kinase C; PLC, phospholipase C; GRKs stands for G-protein-coupled receptor kinases; CREB, Cyclic AMP (cAMP)-response element-binding protein 1; RhoGEFs, Ras homologue guanine-nucleotide exchange factors; RhoA, Ras homologue A; IP3, inositol (1,4,5)-trisphosphate; DAG, diacylglycerol.

$G_{q/11}$ mainly produces and synthesizes the diacylglycerol (DAG) and the inositol triphosphate (IP3), which facilitates efficient production of protein kinase C (PKC), mobilization of calcium ions, and MAPKs like ERK1/2, resulting in the alteration of cell differentiation, adhesion, secretion, growth, and migration. $G_{12/13}$ is the major pathway for the activation of Ras homologue (Rho). G_i and G_{as} are the two main regulators of cAMP (cyclic adenosine monophosphate). The G_i pathway inhibits the production of cAMP via inhibition of adenylyl cyclase (AC), while G_{as} has the opposite effect on the production of cAMP. $G_{\beta\gamma}$ is involved in the regulation of GRKs,

K⁺ channels, and Raf, which is also a key regulator of ERK activation [55, 56]. Except for G-Protein mediating signal transduction, which we have mainly focused on, β -arrestins can also be recruited for the desensitization and internalization of PAR2 [57].

1.4.5 Physiological and pathological roles of PAR2

PAR2 is abundantly distributed in human tissues and cells as mentioned above. It plays critical physiological roles in various systems including the cardiovascular, nervous, immune, respiratory and gastrointestinal systems [41]. In the arteries and veins, membrane-expressed PAR2 on the endothelial and smooth muscle cells contributes to cell proliferation and regulation of vascular tone [58]. In the nervous system, PAR2 is associated with the delivery of nociceptive messages [59]. In the immune system, activation of PAR2 on monocytes may lead to the inflammatory cytokine secretion of IL1 β , IL-6, and IL-8 [60]. In the gastrointestinal tract, PAR2 is involved in the processes of fluid and electrolyte secretion, and the regulation of gastrointestinal motility [61].

Additionally, aberrant activation of PAR2 is relevant in the pathophysiology of several diseases such as metabolic syndrome, cardiovascular disease, arthritis, Immunoglobulin class A (IgA) nephropathy, and cancers [62-69]. Systemic deletion of PAR2 can reduce vascular inflammation in Apolipoprotein E (ApoE) (-/-) mice [62]. In an *in vitro* experiment, the activation of PAR2 on endothelial cells can impair cellular metabolism and lead to insulin resistance due to its pro-inflammatory effect [63]. Inflammatory pathways induced by PAR2 can also be involved in autoimmune diseases including rheumatoid arthritis and IgA nephropathy [64, 65].

Notably, accumulating evidence also strongly suggests a major role of PAR2 in the

angiogenesis of cancers and other conditions [68, 69]. Deletion of PAR2 can delay the appearance of vascularized and invasive carcinoma in an immune competent and spontaneous breast cancer mouse model [68]. And activation of PAR2 can enhance reparative angiogenesis, which results in accelerated hemodynamic recovery and limb salvage in mice [69]. Furthermore, PAR2 is also critical in the development of ischemic stroke. It has been reported that in a murine acute focal cerebral ischemic model, enhanced infarct volume and cell apoptosis were observed at 24 hours of reperfusion when the PAR2 gene had been knocked out [66].

1.5 Autoantibodies targeting GPCR

Natural autoantibodies (NAA) are certain antibodies that react with a wide range of endogenous antigens (e.g., serum proteins, cell surface substances) under physiological or disease conditions [70]. Autoantibodies consist of different classes such as Immunoglobulin class A (IgA), G (IgG), and M (IgM), which differ in their individual levels and antigenic specificity in both normal and pathological conditions [71].

1.5.1 Autoantibodies targeting GPCR in human pathology

Autoantibodies targeting GPCRs have received a lot of attention regarding their role in human pathology. In 1956, autoantibodies targeting the receptor of thyroid-stimulating hormones (TSH) were discovered to be involved in the pathophysiology of Graves' disease [72]. It was reported that neutral or blocking antibodies against TSH receptor, unlike classical stimulating TSHR-Abs, could regulate biased signals in Graves' disease [73]. Subsequently, several other autoantibodies were discovered in other diseases including autoantibodies targeting vascular GPCRs, namely: Angiotensin II type 1 receptor (AT₁R) and Endothelin-1 type A receptor (ET_AR). In 2005, Dragun D. *et al.* provided novel mechanistic

insights into the essential contribution of agonistic AT₁R-Abs targeting AT₁R in antibody-mediated transplant rejection. The group demonstrated that AT₁R-Abs induce the activation of inflammatory cytokine nuclear factor kappa light chain enhancer of activated B cells (NF-κB) via initiating the transcription factor AP-1 [74]. The abnormal presence of AT₁R-Abs and ET_AR-Abs in the serum of patients with systemic sclerosis (SSc) can induce wound repair, chemotaxis, cell proliferation, angiogenesis, thrombosis, and fibrosis through the production of IL-6, IL-8 as well as growth factors [75]. Autoantibodies targeting cardiac β₁-adrenergic receptor (β₁AR) and α₁-adrenergic receptor (α₁AR) are highly associated with cardiomyopathy and refractory hypertension [76].

1.5.2 Autoantibodies against PAR2

PAR2 autoantibodies (PAR2-Abs) isolated from the serum of patients with kidney transplantation could regulate angiogenesis through the production of VEGF [77]. Preliminary clinical data from a collaborative group (PD. Dr. Thomas G. Liman, Department of Neurology, Charité-Universitätsmedizin Berlin, Germany) predicted that PAR2-Abs might function as an independent prognostic factor in ischemic stroke. The group reported that high titers of PAR2-Abs negatively correlate with patient outcome (unpublished data from the group leader, PD. Dr. Thomas G. Liman). However, the mechanistic role of PAR2-Abs in ischemic stroke relative to vascular pathophysiology is unknown.

2. Hypothesis and Objectives

2.1 Hypothesis

PAR2, widely expressed on the membrane of endothelial cells, can regulate the process of angiogenesis, inflammation, and fibrosis. Autoantibodies against PAR2

can modulate PAR2 functions in health and disease. Unpublished clinical data from a collaborative group proved that in patients with ischemic stroke, lower titer PAR2-Abs (quartile 1-3, Q1-3) correlated with a better outcome compared to those in quartile top group (Q4). The hypothesis of this thesis work was that PAR2 IgG isolated from patients with ischemic stroke could affect the production of VEGF by activation of PAR2 and downstream signaling pathways. This work built on previous studies from our laboratory done by Lei Chen and Qing Li [77, 78].

2.2 Objectives

To verify this hypothesis, it was essential to clarify the angiogenesis, G-protein activation and intracellular signaling followed by PAR2-IgG-induced PAR2 activation, and to explore the effects of extracellular loops on G-protein activation as well as the regulatory mechanism of VEGF production. The human endothelial cell line HMEC-1 and human blood-brain barrier cells (hCMEC/D3) were used as model systems to address the following objectives:

1. To study the effects of trypsin and PAR2-IgG on angiogenesis.
2. To detect the G-protein activation, intracellular signaling, extracellular loop functions and PAR2 receptor internalization induced by trypsin and PAR2-IgG.
3. To test the PAR2/ERK-dependent angiogenesis and angiogenic factors.
4. To explore the transcriptional regulatory mechanisms of VEGF triggered by trypsin and PAR2-IgG.
5. To further validate the effect of Q1-3 and Q4 PAR2-IgG on angiogenesis in brain microvascular endothelial cells.

3. Materials and Methods

3.1 Materials

3.1.1 Chemical substances

Reagents	Manufacturer
1 kb DNA ladder	Thermo Fisher Scientific
2-Propanol	Carl Roth
5X Passive Lysis Buffer (PLB)	Promega
10X M-MuLV Reverse Transcriptase Buffer	NEB
10X Trypsin-EDTA	PAA
Acrylamide (37.5:1) Rotiphorese® Gel 30	Carl Roth
Agarose	Serva
Ampicillin	Alkom
Bacto Agar	BD
Bacto Trypton	BD
Bacto Yeast Extract	BD
Bis-Tris	AppliChem
BSA	Carl Roth
Chloroform	Carl Roth
Diethyl pyrocarbonate (DEPC)	Sigma Aldrich
Dimethyl sulfoxide (DMSO)	Sigma Aldrich
Dithiothreitol (DTT)	AppliChem
DMEM Low glucose medium	Biowest
DNA Gel Loading Dye (6X)	Thermo Fisher

Reagents	Manufacturer
dNTP mix	Thermo Fisher Scientific
Dulbecco's Phosphate Buffered Saline (PBS)	Biochrom
Ethanol 99.8%	Carl Roth
Ethylenediaminetetra-acetic acid (EDTA)	Carl Roth
FastStart Universal SYBR Green Master	Roche
Fetal calf serum (FCS)	Gibco
FSLLRN-NH ₂ trifluoroacetate salt	Sigma Aldrich
Gelatin	Sigma
Glycerin	Carl Roth
hEGF	Sigma Aldrich
Hydrocortisone	Sigma Aldrich
L-Glutamine	PAA
MCDB-131	c.c. pro GmbH
Midori Green Advance DNA Stain	NIPPON Genetics
M-MuLV Reverse transcriptase (200,000 U/mL)	NEB
MOPS	AppliChem
NaF (Sodium Fluoride)	AppliChem
Nonfat dried milk powder	AppliChem
Oligo d(T) 16	Invitrogen
PD 184352	Sigma Aldrich
Penicillin-Streptomycin Solution 100X	Biowest
Ponceau S	Carl Roth

Reagents	Manufacturer
Protease Inhibitor Tablets, Complete Mini	Roche Applied Science
Protein Marker VI (10-245) prestained	AppliChem
PVDF (polyvinylidene difluoride)	GE Healthcare
RNase inhibitor	Thermo Fisher Scientific
Roche complete inhibitor	Roche Diagnostics GmbH
SOC Medium	Clontech
Sodium azide	Sigma Aldrich
Sodium chloride	Carl Roth
Sodium dodecyl sulfate (SDS) Pellets	Carl Roth
Sodium hydroxide	Sigma Aldrich
Sodium orthovanadate (Na ₃ VO ₄)	Roth
Sodium pyrophosphate	AppliChem
SuperSignal West Dura	Thermo Scientific
SuperSignal West Pico	Thermo Scientific
Tris	Carl Roth
Tris-HCl	Sigma Aldrich
TritonX-100	Sigma Aldrich
Trypan blue	Sigma Aldrich
Trypsin from bovine pancreas	Sigma Aldrich
Tween 20	Sigma Aldrich
WesternBright Sirius HRP substrate	Advansta

3.1.2 Equipment

Equipment	Manufacturer
Applied Biosystems® 7500 Real-Time PCR System	Thermo Fisher Scientific
Axiovert 40 CFL Microscope	Carl Zeiss
Biofuge primo R	Thermo Fisher Scientific
Digital Heatblock II	VWR
Duomax 1030 Platform Shaker	Heidolph Instruments
Electrophoresis Power Supply Model EPS-3500	Pharmacia Biotech
FLUOstar OPTIMA Microplate Reader	BMG LABTECH
FRESCO 21 Centrifuge	Thermo Electron Corporation
Gel documentation system	VWR
HERA cell 240 Incubator	Thermo Electron Corporation
HERA safe Microbiological Safety Cabinet	Thermo Electron Corporation
Heraeus / BB 6220 CU O ₂	Thermo Fisher Scientific
Incubating Orbital Shaker professional 3500	VWR
Model 200/2.0 POWER SUPPLY	Bio-Rad
Multiskan Ascent 354 Microplate Reader	Thermo Fisher Scientific
ND-1000 Spectrophotometer	VWR
Perfusor segura FT	Braun
Polymax 1040 T Platform Shaker	Heidolph
Rotor RS-TR05	Phoenix Instrument
SUB Waterbath	Grant
T Professional BASIC XL 96 Thermocycler	Biometra

3.1.3 Kits

Kits	Manufacturer
Direct-zol™ RNA MiniPrep	Zymo Research
Buffer Kit for Antibody Pairs	Invitrogen
DC™ Protein Assay	Bio-Rad
Dual-Luciferase® Reporter Assay System	Promega
Nano-GLO® HiBiT Extracellular Detection System	Promega
GeneJET Plasmid Miniprep Kit	Thermo Fisher Scientific
HiTrap Protein G HP	GE Healthcare
In-Fusion® HD Cloning Kit	Takara
Luciferase Assay System	Promega
IL-6 Human ELISA Kit	Invitrogen
IL-8 Human ELISA Kit	Invitrogen
Angiopoietin 2 Human ELISA Kit	Invitrogen
Human GRO α Uncoated ELISA Kit	Invitrogen
Human VEGF Standard TMB ELISA Kit	PeproTech
NucleoBond®Xtra Midi/Maxi	Takara
NucleoBond®Xtra Midi/Maxi EF	Takara
PeqGOLD MicroSpin Cycle pure Kit	PEQLAB
Q5® Site-Directed Mutagenesis Kit	New England BioLabs
EndoGRO™-MV-VEGF Complete Media Kit	Merck Millipore
Xfect Transfection Reagent	Takara

3.1.4 Plasmid, bacteria, cell lines and enzymes

Plasmid	Manufacturer
pcDNA3.1+ vector	Invitrogen
pGL4.33(luc2P/SRE/Hygro) vector	Promega
pGL4.34(luc2P/SRF-RE/Hygro) vector	Promega
pGL4.30(luc2P/NFAT-RE/Hygro) vector	Promega
pRL Renilla Luciferase Control Reporter Vector	Promega
pcDNA-PAR2	Taken from Lei Chen [77]
pcDNA-PAR2 ECL1 Ala	Taken from Qing Li [78]
pcDNA-PAR2 ECL2 Ala	Taken from Qing Li [78]
pcDNA-PAR2 ECL3 Ala	Taken from Qing Li [78]
VEGF 5'-deletion luciferase plasmids (pLuc 2068, pLuc 1340, pLuc 840, pLuc 435, and pLuc 102)	Provided by A. Scholz

Bacteria	Manufacturer
NEB 5-alpha Competent E.coli Cells	New England BioLabs
Stellar competent Cells	Takara

Cell lines	Provider
Human microvascular endothelial cells (HMEC-1)	ATCC
Human cerebral endothelial cells (HCMEC/D3)	Sigma Aldrich

Enzymes and provided buffer	Manufacturer
<i>Hind</i> III-HF	
<i>Bam</i> HI-HF	
<i>Eco</i> RI-HF	New England BioLabs
<i>Xho</i> I	
CutSmart Buffer	

3.1.5 Antibodies

Antibodies	Company	Dilution
Akt antibody (# 9272)	Cell signaling	1:1000
GAPDH antibody (# 6C5CC)	HyTest	1:10000
p44/42 MAPK (Erk1/2) antibody (# 9102)	Cell signaling	1:1000
Peroxidase-conjugated Anti-Mouse IgG	AffiniPure Donkey Dianova	1:15000
Peroxidase-conjugated Anti-Rabbit IgG	AffiniPure Donkey Dianova	1:15000
Phospho-Akt (Ser473) antibody (# 9271)	Cell signaling	1:1000
Phospho-p44/42 MAPK (Erk1/2) (Thr202/Tyr204) antibody (#9106)	Cell signaling	1:1000

3.1.6 Buffer recipes

Buffer	Reagent	Final conc.
	BICIN	25 mM
BICIN transfer buffer 1x	Bis-Tris	25 mM
	EDTA, pH 8.0	1 mM
	Ethanol	10% v/v

Buffer	Reagent	Final conc.
Blocking buffer (WB)	Nonfat dried milk powder	5% m/v
	BSA	1% m/v
	Add 1x TBS-T	
Gel buffer 3.5x, pH 6.5-6.8	Bis-Tris	1.25 M
Gelatin stock solution	Gelatin	2% m/v
	In PBS	
	Sterilized by autoclaving	
Laemmli buffer 5x	Tris-HCl, pH 7.5	250 mM
	DTT	500 mM
	Glycerol	30% v/v
	SDS	5% m/v
	Bromphenol blue	0.25% m/v
MOPS running buffer 1x,	pH 7.7 MOPS	50 mM
	Tris	50 mM
	EDTA, pH 8.0	1 mM
	SDS	0.1% m/v
PBS (Ca ²⁺ -/Mg ²⁺ -free), pH 7.3	NaCl	137 mM
	KCl	2.7 mM
	Na ₂ HPO ₄	9 mM
	KH ₂ PO ₄	2.3 mM
Striping buffer (WB), pH 6.7	Tris	62.5 mM
	SDS	2% m/v
TBE buffer 1x, pH 8.0	Tris	89 mM
	Boric acid	89 mM

Buffer	Reagent	Final conc.
	EDTA	2 mM
TBS-T buffer 1x, pH 7.6-8.0	Tris	50 mM
	NaCl	150 mM
	Tween 20	0.1% v/v
TE buffer 10X	Tris-HCl, pH 7.5	0.1 M
	EDTA	0.01 M
TST buffer	Tris-HCl, pH 8.0	100 mM
	SDS	0.2% m/v
	TritonX-100	1% v/v
TST lysis buffer (WB)	TST buffer	
	100x Complete with EDTA @Roche	1X
	100 mM NaOrV (Sodium ortho vanadate)	1 mM
	1 M β -Glycerophosphate	10 mM
	500 mM NaF	5 mM
	0.1 M Natriumpyrophosphate	1 mM
Wash buffer (ELISA)	Tween 20	0.05%
	Add 1x PBS	

3.1.7 Media

Buffer	Reagent	Final conc.
HCMEC/D3 complete medium	EndoGRO TM -MV-VEGF Complete Media Kit	5% FBS
HCMEC/D3 starvation medium	EndoGRO TM -MV-VEGF Complete Media Kit	0.5% FBS
HMEC-1 complete medium	L-glutamine	10 mM

Buffer	Reagent	Final conc.
	hEGF	10 ng/mL
	Hydrocortisone	10 nM
	FCS	5% v/v
	Penicillin	100 U/mL
	Streptomycin	100 µg/mL
	L-glutamine	10 mM
HMEC-1 starvation medium	hEGF	10 ng/mL
	Hydrocortisone	10 nM
	FCS	0.5% v/v
	Penicillin	100 U/mL
	Streptomycin	100 µg/mL
	L-glutamine	10 mM
HMEC-1 serum-free medium	hEGF	10 ng/mL
	Hydrocortisone	10 nM
	Penicillin	100 U/mL
	Streptomycin	100 µg/mL
	Bacto tryptone	1% m/v
LB agar plate	Bacto yeast extract	0.5% m/v
	NaCl	1% m/v
	Bacto agar	1.5% m/v
	sterilized by autoclaving	
	Bacto tryptone	1% m/v
LB medium	Bacto yeast extract	0.5% m/v
	NaCl	1% m/v

Buffer	Reagent	Final conc.
	sterilized by autoclaving	

3.1.8 Primers

Mutagenic primers were designed and analyzed using the NEBaseChangerTM software online. Primers (Biolegio company) for mutant generation, sequencing and quantitative real-time PCR (qRT-PCR) are listed in Tables 1, 2 and 3, respectively.

Constructs name	5'- to -3'
pcDNA-PAR2-HiBiT-Tag	Forward: GAAGATTAGCGGAAGTTCAGGTGATGGCACATCCCACGTC
	Reverse: TTGAACAGCCGCCAGCCGCTCACAACCTTACCAATAAGGC TTCTTC

Table 1. Primers for mutant generation

Sequencing primers	5'- to -3'
pcDNA cmv (from nucleotides from 769 to 789)	Forward: CGCAAATGGGCGGTAGGCGTG

Table 2. Primers for sequencing

Primers for qRT-PCR	5'- to -3'
Human GAPDH se	CATCACCATCTTCCAGGAGCG
Human GAPDH ase	TGACCTTGCCCACAGCCTTG
Human B2M se	GTGCTCGCGCTACTCTCTCT
Human B2M ase	CGGCAGGCATACTCATCTTT
Human PAR2 se	CGTCCAGTGGAGCTCTGAGT
Human PAR2 ase	GGGATGTGCCATCAACCTTA
Human VEGFA se	CCTTGCTGCTCTACCTCCAC
Human VEGFA ase	CACACAGGATGGCTTGAAGA

Human CXCL1 se	AGGGAATTCACCCCAAGAAC
Human CXCL1 ase	TAACTATGGGGGATGCAGGA
Human IL-6 se	TACCCCCAGGAGAAGATTCC
Human IL-6 ase	AGTGCCTCTTTGCTGCTTTC
Human IL-8 se	GTGCAGTTTTGCCAAGGAGT
Human IL-8 ase	CTCTGCACCCAGTTTTTCCTT
Human ANG2 se	GCAAGTGCTGGAGAACATCA
Human ANG2 ase	CACAGCCGTCGTGTTCTGTA

Table 3. Primers for quantitative real-time PCR

3.2 Methods

3.2.1 RNA extraction, cDNA production and qRT-PCR

3.2.1.1 RNA extraction

Briefly, RNA extraction from HMEC-1 in the exponential growth phase was performed using the Qiazol Lysis Reagent according to the manufacturer's protocol. Other procedures were performed as detailed previously [77].

3.2.1.2 Agarose gel electrophoresis

TBE agarose gel (1%) was prepared and placed into TBE buffer for agarose gel electrophoresis. Samples were mixed with 1:50 Midori green Advance DNA Stain and 6X DNA loading buffer. DNA ladder and RNA samples were loaded into wells and electrophoresed for one hour at 100V, followed by bands imaging under a UV-transilluminator.

3.2.1.3 cDNA production

500 ng of RNA template was used to synthesize cDNA by reverse transcription polymerase chain reaction (RT-PCR) with reverse transcriptase and primers. The

RT-PCR components are listed in Table 4, and the reaction conditions in Table 5.

Content	Final conc.
10X M-MuLV Reverse transcriptase Buffer	1X
dNTP mix 10 mM	1.6 mM
RNase inhibitor	0.8 U/ μ L
M-MuLV Reverse transcriptase 200,000 U/mL	1 U/ μ L
Oligo	1 μ M
RNA	0.01 μ g/ μ L
Total	50 μ L

Table 4. cDNA synthesis components

Temperature (°C.)	Time
25	10 min
42	45 min
95	5 min
4	indefinite

Table 5. RT-PCR reaction conditions

3.2.1.4 qRT-PCR

The expression of the targeted genes was quantified by qRT-PCR with the Applied Biosystems® 7500 System under the two-step cycling program listed in Table 6. qRT-PCR components are shown in Table 7.

Temperature (°C.)	Time
90	10 min

60	1 hour	40 cycles
90	5 min	
4	indefinite	

Table 6. qRT-PCR program

Content	Volume (1X)	Final conc.
SYBR Green	6.5 μ L	1X
Primer se 10 μ M	0.5 μ L	0.4 μ M
Primer ase 10 μ M	0.5 μ L	0.4 μ M
ddH ₂ O	4.5 μ L	--
cDNA	1 μ L	--
Total	13 μ L	--

Table 7. qRT-PCR components

3.2.2 Generation of PAR2-HiBiT constructs

3.2.2.1 Site-directed mutagenesis

The HiBiT tag was cloned into the N-terminus of PAR2 using the Q5[®] Site-Directed Mutagenesis Kit following the instructions. Briefly, the pcDNA3-PAR2-HiBiT cDNA fragment was amplified using High-Fidelity DNA Polymerase and the specific primers shown in Table 1. The reaction components and conditions of the PCR are shown in Tables 8 and 9, respectively.

Component	Volume	Final conc.
Q5 Hot Start High-Fidelity 2X Master Mix	12.5 μ L	1X
10 μ M Forward Primer	1.25 μ L	0.5 μ M

Component	Volume	Final conc.
10 μ M Reverse Primer	1.25 μ L	0.5 μ M
Template cDNA (PAR2)	1 μ L	10 ng
Nuclease-free Water	9.0 μ L	--

Table 8. Mutagenesis reaction components

Step	Temperature ($^{\circ}$C.)	Time	
Initial Denaturation	98	30 s	
Second Denaturation	98	10 s	35 cycles
Annealing	68	30 s	
Elongation Step	72	6 min	
Final Extension	72	5 min	
Hold	4		

Table 9. Mutagenesis PCR reaction conditions

The second step involved incubation with the KLD enzyme mix provided in this kit. Together, these enzymes of the reaction system participate in the rapid circularization of PCR products and excision of DNA template (Table 10).

Components	Volume	Final conc.
PCR Product	1 μ L	--
2X KLD Reaction Buffer	5 μ L	1X
10X KLD Enzyme Mix	1 μ L	1X
Nuclease-free Water	3 μ L	--

Table 10. KLD reaction system

3.2.2.2 Bacterial transformation

In brief, the mixture of KLD product (5 µL) and 5- α -Competent *E. coli* (50 µL) was incubated under the following three steps: 1) on ice for 30 minutes; 2) heat shock at 42°C for 45 seconds; 3) 5 minutes incubation on ice. The other procedure was performed as detailed previously [77].

3.2.2.3 Plasmid isolation and sequencing

A single colony was picked and cultured for further plasmid isolation. The procedure was performed as detailed previously [77]. A suitable quantity of plasmids was then sequenced using the primers listed in Table 2 at the LGC Genomics GmbH company. The results were analyzed using the NCBI nucleotide BLAST tool.

3.2.2.4 Bacterial glycerol stock

250µl of the above-mentioned pre-cultured bacterial mixture was mixed thoroughly with 750µl of 60% glycerol and frozen at -80°C.

3.2.3 Patient IgG isolation

In this study, IgG was isolated from frozen sera of patients in the ‘PROSpective Cohort with Incident Stroke Berlin’ (PROSCIS-B; NCT01363856), a prospective observational hospital-based cohort of patients after their first-ever stroke. Each patient, or their legal representative, give written informed consent to participate in the study. The PROSCIS-B study was approved by the Ethics Committee of the Charité–Universitätsmedizin Berlin (EA1/218/09) and was conducted according to ethical principles within the framework of the Declaration of Helsinki. Blood samples from patients with ischemic stroke were collected once at any time within seven days after admission. 489 ischemic stroke patients with clinical information on baseline, PAR2-IgG levels and functional outcome at one year were included. Levels of PAR2 autoantibodies in the serum were measured with a sandwich Elisa by CellTrend GmbH. Unpublished clinical data analyzed by the group (PD. Dr. Thomas G Liman)

we collaborated with showed that patients with levels of PAR2-IgG in the top quartile (above 14 U/mL, Q4), when compared to all other patients with a PAR2-IgG level below 14 U/mL (Q1-3), were at increased risk of poor outcome after adjusting by age, sex, etiological subtypes, stroke severity, pre-stroke dependency, and vascular risk factors (OR 2.0, 95%CI 1.2-3.4). The serum was divided into 2 groups (Q1-3, Q4), and 2 individual sera in each group were pooled for IgG isolation. Briefly, IgGs were isolated from serum by affinity chromatography with HiTrap Protein G columns, which was detailed previously [77].

3.2.4 Cell culture and stimulation

3.2.4.1 HMEC-1 and Blood-Brain Barrier hCMEC/D3 culture

HMEC-1 and hCMEC/D3 frozen in liquid nitrogen were thawed rapidly in a 37°C water bath, then added into 5 mL of complete medium and lastly centrifuged. After resuspension in complete medium, cells were seeded into a 0.2% gelatin pre-coated flask and cultured at 37°C.

Cells at about 80%-90% confluence were processed with 2 mL trypsin-EDTA followed by neutralization with 10 mL complete medium. The number of live cells was measured by the trypan blue dye exclusion test. The number of cells seeded per well in different plates or flasks is shown in Table 11.

Container Type	Number of HMEC-1	Number of hCMEC/D3
96-well plate	5,000	5,000
24-well plate	50,000	50,000
12-well plate	100,000	100,000
6-well plate	200,000	200,000
6 cm ² flask	500,000	500,000
75 cm ² flask	1,000,000	1,000,000

Table 11. Initial number of cells in different cell culture vessels

3.2.4.2 Cell stimulation

Cells at 70% confluence were treated with starvation medium overnight before addition of stimuli. For ELISA, cells were stimulated with trypsin (100 nM, 6 hours) or IgG (1 mg/mL, 6 hours), and then the supernatant was collected. For mRNA expression analysis, cells were stimulated for different times depending on the target genes. For pathway blocking assays, cells were pre-incubated with PAR2-blocker (FSLRLRY-NH₂ trifluoroacetate salt, 100nM), as well as ERK-blocker (PD184352, 0.1µM, 1.0µM, 10µM) for one hour followed by stimulation as previously described.

3.2.5 Matrigel angiogenesis assay

HMEC-1 or hCMEC/D3 at 80%-90% confluence were processed as detailed in section 3.2.4.1, and prepared for further use. The cells were diluted and adjusted to a concentration of 2.0×10^5 /mL with serum-free medium.

IgG samples were diluted with 5% FCS DMEM medium to a concentration of 2.0 mg/mL. 100µL of cell suspension was mixed thoroughly with 100 µL of IgG solution. The final 200µL were then added on top of the matrigel uniformly. The formation of capillary-like tubes of endothelial cells was observed and photographed under the microscope after 16 hours of incubation. The images (magnification 100X) were analyzed with the "Angiogenesis Analyzer" add-on from Image J [79]. Total length/Field, i.e., the total length of the detected master segments adjusted by the field area, was the main indicator to represent the capacity of endothelial cells to form tubes.

3.2.6 Luciferase reporter assay

Cells at 70% confluency were transfected with appropriate plasmids using the Xfect transfection reagent under the manufacturer's instructions. In a 24-well plate, HMEC-1 was transiently co-transfected with Nucleated Factor of Activated T-Cells (NFAT, 200 ng), Serum Response Element (SRE, 100 ng), or Serum Response Factor (SRF, 100 ng) reporter plasmid together with 200 ng of pcDNA-PAR2 plasmid per

well, and then cultured with starvation medium for 4 hours, followed by complete medium for 24 hours. After 6 hours of stimulation with trypsin, PAR2-IgG, or DMEM low glucose, cells were washed with PBS twice prior to a 15 minute lysis with 1X PLB under constant shaking. The Luciferase Assay System (LAS) from Promega was used to assess luciferase activity of cell lysates, using a FLUOstar microplate reader under the manufacturer's instructions.

3.2.7 Nano-GLO[®]HiBiT Extracellular Detection assay

HMEC-1 was seeded into each well of a 96-well plate, and was cultured for 3 days. After transfection with 50 ng pcDNA-PAR2-HiBiT plasmid, the cells were stimulated with trypsin for 20 minutes and PAR2-IgG for 6 hours. After stimulation, cells were washed twice. Finally, each well was incubated with 100 μ L of Nano-Glo[®]HiBiT Extracellular Reagent mixture for 10 minutes before measuring luminescence with a FLUOstar microplate reader under the manufacturer's instructions.

3.2.8 Dual luciferase reporter assay

Here, 400 ng of VEGF2068 promoter-luciferase plasmid or truncated VEGF promoter plasmids [80] and 20 ng of Renilla reference vector were co-transfected in 12-well plates with Xfect transfection reagent following the manufacturer's instructions. After 4 hours of transfection in starvation medium, the medium was changed to complete medium for 24 hours. Following 6 hours of stimulation with trypsin, PAR2-IgG, or DMEM low glucose (control), cells were washed twice before being lysed with 1X PLB for 15 minutes under constant shaking. The Luciferase activity of lysates was assessed using the LAS from Promega with a FLUOstar microplate reader. After the addition of stop solution into cell lysates, the Renilla reference activity was assessed.

3.2.9 Western blot

HMEC-1 was stimulated with trypsin and IgG for 15 minutes and scraped off. Next, the procedure of protein isolation and western blot was done, as detailed previously

[77]. All antibodies we applied in this section are shown in the Antibodies section above.

3.2.10 ELISA

The concentration of IL-6, IL-8, VEGF, CXCL1, and ANG2 in the cell supernatants were measured with ELISA Kits from Invitrogen under the manufacturer's instructions. Briefly, various capture antibodies were coated onto each well provided in ELISA Kits at 4°C overnight. 100 µL of standards, control, and supernatant samples were measured in duplicate. Detection antibodies and Streptavidin-HRP solution were used to conjugate with antigens. Reaction systems were incubated with Stabilized Chromogen for 30 minutes until the solution turned blue, and were then stopped with stop solution. Absorbance of targeted proteins at 450 nm (reference absorbance: IL-6, IL-8, VEGF, ANG2 630 or CXCL1 570 nm) was measured in 5 minutes with the Thermo Multiskan Ascent 96 plate reader. The standard curve was plotted, and then the concentration of samples was calculated according to linear regression.

3.2.11 Statistical analysis

Data are expressed as mean \pm SEM, n stands for the number of independent experiments in each group. Comparisons of two groups were performed by t-test or Wilcoxon test, comparisons between more than 3 groups were performed by one-way ANOVA (normal distribution) or Kruskal-Wallis test, and two-way ANOVA including Turkey's multiple comparison test was used to compare groups with two different independent variables. Differences were considered to be significant when the *p*-value of a one-tailed test was less than 0.05. GraphPad Prism software (version 8.0) was used for the statistics.

4. Results

4.1 Trypsin- and PAR2-IgG-induced angiogenesis in HMEC-1

As mentioned in Methods section 3.2.3, unpublished clinical data from PD. Dr. Thomas G. Liman demonstrated that PAR2-IgG was related to the outcome of stroke patients. However, the functions and mechanisms for this observation are unclear. To determine the effects of PAR2-IgG in modulating PAR2 signaling, and thus the resulting angiogenesis, PAR2-IgG stimulation was compared with the PAR2 natural agonist trypsin [44]. Human microvascular endothelial cells, HMEC-1, which highly express PAR2, were used in this study [77].

4.1.1 Trypsin and Q1-3 PAR2-IgG increased angiogenesis in HMEC-1

Angiogenesis is an important process that influences the outcome in the acute phase of ischemic stroke [10]. Thus, matrigel tube formation assay was applied to explore the *in vitro* effects of trypsin and PAR2-IgG on angiogenesis. As depicted in Figure 3A, there was an up-regulation of endothelial angiogenesis *in vitro* after trypsin stimulation in a dose-dependent manner. 100nM demonstrated statistically significant effects and this concentration was thus used in the following experiments. In Figure 3B, cells treated with Q1-3 PAR2-IgG (1mg/mL) show significant higher tube formation, and hence increased angiogenesis, when compared to DMEM ($p<0.05$) and Q4 PAR2-IgG (1mg/mL) ($p<0.01$).

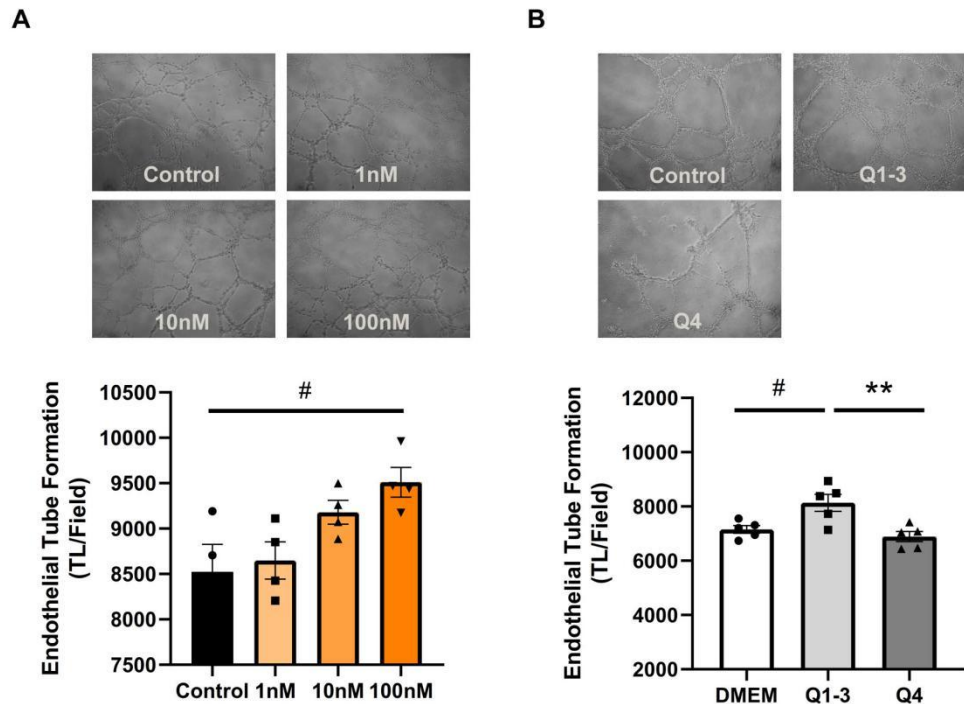


Figure 3. Effects of trypsin and PAR2-IgG on endothelial cell tube formation. HMEC-1 were stimulated with (A) 1nM, 10nM, 100nM trypsin (n=4) or (B) Q1-3- and Q4-PAR2-IgG (1mg/mL) (n=5). Representative phase-contrast images (magnification 100X) are presented in the upper panels. The graphs below show quantifications of 4 or 5 independently performed experiments. The capacity of tube formation was assessed by a main indicator of total length of the detected master segments adjusted by field area after 16 hours. * $p < 0.05$ and ** $p < 0.01$ compare between treated groups, # $p < 0.05$ compares to control group. Values are presented as individual data points together with bars with mean \pm SEM.

4.1.2 Angiogenic genes involved in trypsin-induced tube formation

Having established that Q1-3 PAR2-IgG and trypsin promote angiogenesis, angiogenic genes were explored, which might be involved in vascular tube formation, such as *VEGF*, *IL-6*, *IL-8*, *CXCL1* and *ANG2* [16-20].

4.1.2.1 Optimization of trypsin stimulating time on angiogenic genes

100nM trypsin was used to assess the transcriptional regulation of the selected genes in a time-dependent manner. As shown in Figure 4, there was a significant

transcription up-regulation of *VEGF*, *IL-6*, *IL-8*, and *CXCL1* after 1 hour, which did not last. *ANG2* showed an increase in mRNA levels only after 3 hours, with a peak at 6 hours.

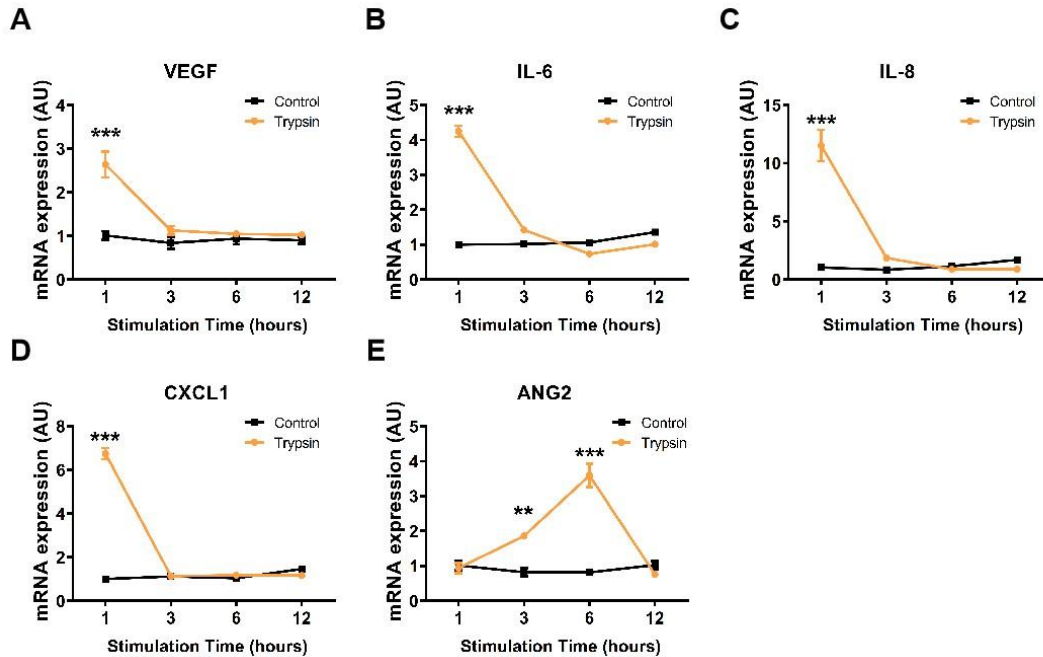


Figure 4. Time-dependent increase of endothelial angiogenic gene expressions in response to trypsin. HMEC-1 were stimulated with 100nM trypsin for different time periods and then the angiogenic genes (A) *VEGF*, (B) *IL-6*, (C) *IL-8*, (D) *CXCL1*, and (E) *ANG2* were quantitatively measured by qRT-PCR. *P<0.05, **P<0.01, ***P<0.001 vs unstimulated control group, n=3. Data are presented as bars with mean \pm SEM.

4.1.2.2 Trypsin increased dose-dependent angiogenic gene transcription

Increases in gene transcription were further investigated using different doses of trypsin at the previously explored peak expression times. Concordantly to the matrigel experiment, 100 nM trypsin produced a significant up-regulation in the examined angiogenic gene expression compared to other concentrations of trypsin. Trypsin concentrations of 1 and 10nM had no to minimal effect on these angiogenic gene expression levels (Figure 5).

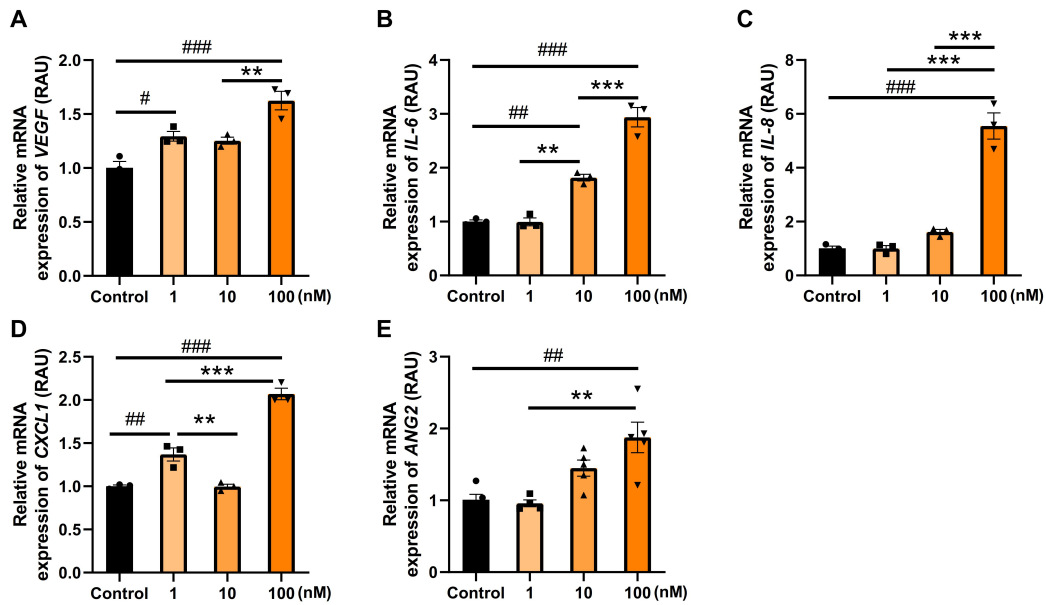


Figure 5. Trypsin increased dose-dependent angiogenic genes transcription. HMEC-1 were stimulated with 1, 10 or 100nM trypsin, and the angiogenic genes including (A) *VEGF*, (B) *IL-6*, (C) *IL-8*, and (D) *CXCL1* were assessed after 1 hour, or in the case of (E) *ANG2* 6 hours. ** $p < 0.01$, *** $p < 0.001$ compare between treated groups; # $p < 0.05$, ## $p < 0.01$, ### $p < 0.001$ compare to control group, $n = 3$. Data are presented as individual data points together with bars with mean \pm SEM.

4.1.2.3 Trypsin increased dose-dependent angiogenic cytokine release

Further analyses were performed to assess how trypsin influenced angiogenic cytokine release. Protein levels in cell supernatants were determined and showed dose-dependent releases when compared with unstimulated controls. Protein levels of VEGF, IL-6, IL-8, CXCL1, and ANG2 in the supernatants from HMEC-1 treated with 100nM trypsin were significantly higher than those from unstimulated cells (Control), and 1 or 10 nM doses of trypsin treated cells (except for VEGF). 1 and 10 nM doses of trypsin had no to minimal effect on protein release (Figure 6).

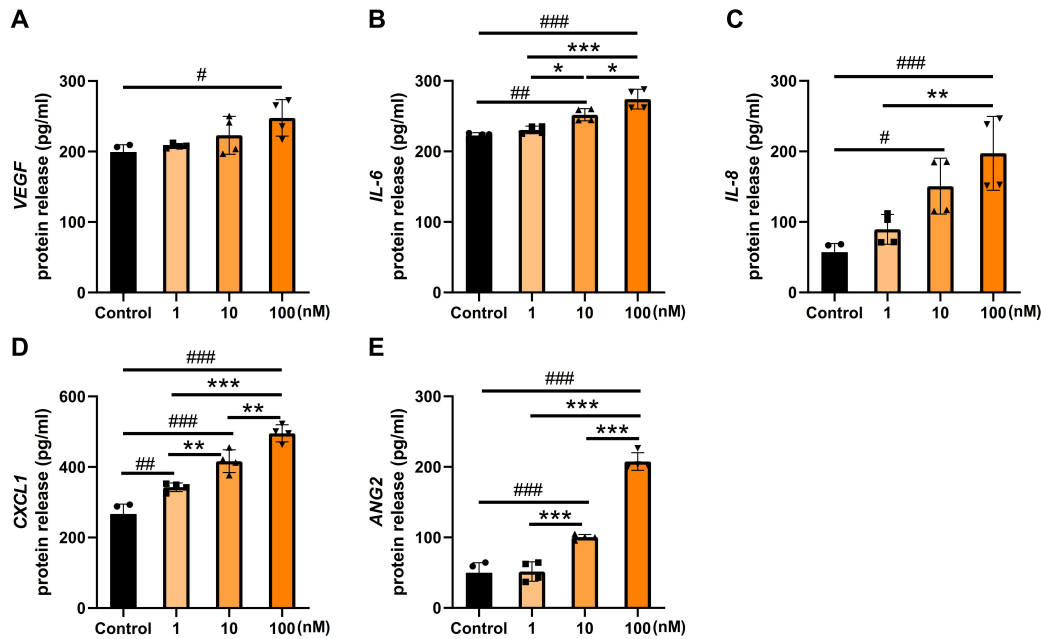


Figure 6. Trypsin increased dose-dependent angiogenic cytokine release. Cell supernatants were collected after 6 hours stimulation with 1, 10 and 100nM trypsin and then the angiogenic cytokine release including (A) *VEGF*, (B) *IL-6*, (C) *IL-8*, (D) *CXCL1*, and (E) *ANG2* were measured by ELISA. * $p < 0.05$, ** $p < 0.01$, *** $p < 0.001$ compare between treated groups; # $p < 0.05$, ## $p < 0.01$, ### $p < 0.001$ compare to control group, $n = 4$. Data are presented as individual data points together with bars with mean \pm SEM.

In conclusion, trypsin increased angiogenic gene transcription after 1 hour, except for *ANG2* with a somewhat later peak, and the respective protein releases after 6 hours.

4.2 PAR2 induced G-protein activation and intracellular ERK1/2 signaling

Next, the angiogenic signaling and molecular mechanisms of PAR2 activation induced by PAR2-IgG were explored.

4.2.1 G-protein activation of PAR2 by Q1-3 and Q4 PAR2-IgG

Activation of G-protein α subunits is crucial for initiating various downstream pathways and regulating gene transcription. Our group has previously reported that

trypsin could activate $G_{q/11}$, $G_{\alpha_{12/13}}$ and ERK1/2 [77]. However, the effects of PAR2-IgG on G-protein subtypes are still unknown. Luciferase reporter assay, which incorporates transcriptional factors specific to cognate G_{α} , is widely used to monitor G-protein activation, as shown in Figure 7 [81]. This assay system was used to monitor the activation of G-protein subtypes $G_{q/11}$ (NFAT), $G_{\alpha_{12/13}}$ (SRF) and ERK1/2 (SRE) in mammalian cells when stimulated with trypsin or PAR2-IgG.

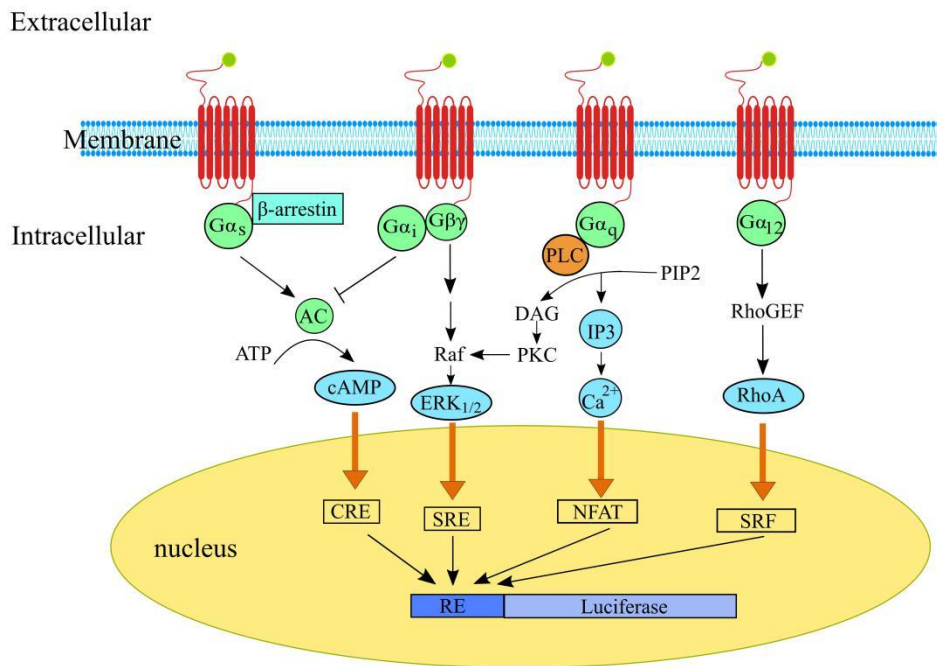


Figure 7. Schematic overview of major GPCR signaling pathways and relevant response elements.

(Modified from Fig.1, [81]). AC, Adenylyl cyclase; cAMP, Cyclic adenosine 3',5'-monophosphate; PKA, protein kinase A; PKC, protein kinase C; PLC, phospholipase C; RhoGEF, Ras homologue guanine-nucleotide exchange factor; RhoA, Ras homologue A; IP3, inositol (1,4,5)-trisphosphate; DAG, diacylglycerol; CRE, Cyclic AMP (cAMP)-response element; SRE, Serum Response Element; NFAT, Nucleated Factor of Activated T-Cells; SRF, Serum Response Factor.

As shown in Figure 8, Q1-3 PAR2-IgG significantly increased (A) $G_{q/11}$ and (B) ERK1/2 activity by 122.0% ($p < 0.01$) and 103.0% ($p < 0.01$), respectively, when compared with the control group. Upon stimulation with Q4 PAR2-IgG, (A) $G_{q/11}$ and (B) ERK1/2 activity showed nonsignificant increases by 34.5% and 36.1%, respectively. Conversely, (C) no $G_{\alpha_{12/13}}$ activation was observed when stimulated with

either Q1-3 or Q4 PAR2-IgG.

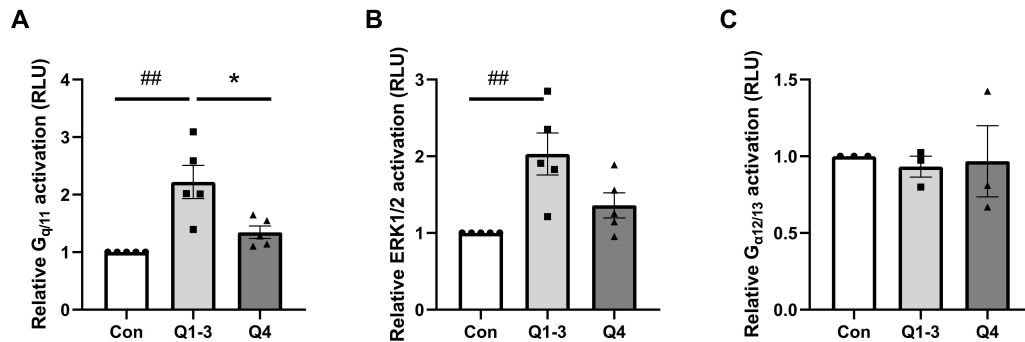


Figure 8. Effects of PAR2-IgG on $G_{q/11}$ or $G_{\alpha 12/13}$ and ERK1/2 activation. HMEC-1 were stimulated with Q1-3- or Q4-PAR2-IgG (1mg/mL). Endothelial (A) $G_{q/11}$, (B) ERK1/2, or (C) $G_{\alpha 12/13}$ (n=3) activation was assessed after 6 hours. * $p < 0.05$ compares between treated groups; ## $p < 0.001$ compares to control group, n=5. Values are presented as individual data points together with bars with mean \pm SEM.

4.2.2 Trypsin time- and dose-dependently induced endothelial

ERK1/2 and Akt signaling

Additionally, the signaling dynamics of PAR2 following trypsin activation were investigated. Our laboratory has previously shown that trypsin activated ERK1/2 [77]. PAR2 also activates the Akt signaling pathway in various cell lines [82]. The activation of ERK1/2 and Akt were investigated using western blotting in a time- and dose-dependent manner. As shown in Figure 9, the phosphorylation of (A) ERK1/2 and (C) Akt at Ser 473 position showed an increase at 5 minutes, reached a peak at 15 minutes, and then decreased sharply to a level comparable to that of 5 minutes. At 15 minutes, there was a higher activation of ERK1/2 (Figure 9B) and Akt (Figure 9D), with a mean value of 3.3-fold and 11.1-fold ($p < 0.05$), respectively, in response to 100nM trypsin when compared to control group.

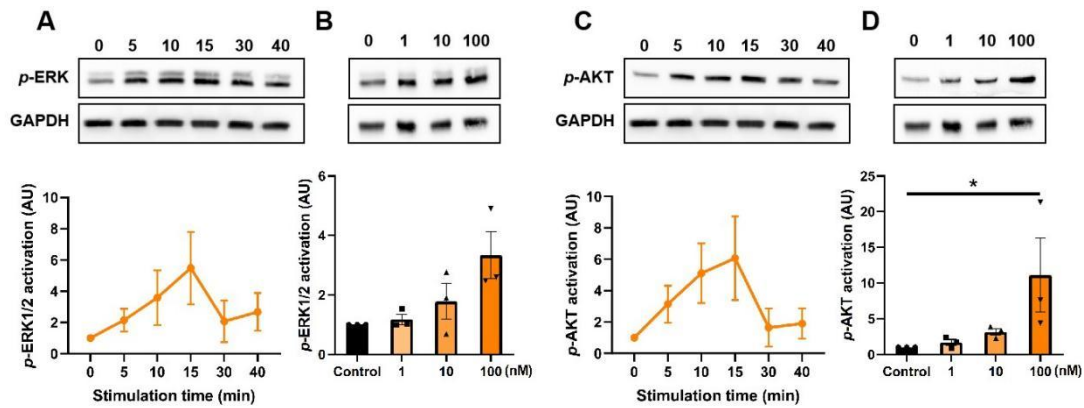


Figure 9. Time- and dose-dependent trypsin-induced endothelial ERK1/2 and Akt activation. (A, C). HMEC-1 were treated with 100nM trypsin for 0 to 40 minutes for time-dependent analysis of ERK1/2 and Akt activation. (B) Endothelial ERK1/2 and (D) Akt activation were assessed after 15 minutes stimulation with doses of 1, 10 and 100nM trypsin. ERK1/2 and Akt activation were normalized to GAPDH. * $p < 0.05$ vs control group, $n = 3$. Values are presented as individual data points together with bars with mean \pm SEM.

4.2.3 Q1-3 PAR2-IgG induced stronger endothelial ERK1/2 and Akt signaling

The previous results have shown that trypsin induced increased activation of ERK1/2 and Akt. The effects of PAR2-IgG on these signaling pathways were then investigated. As depicted in Figure 10, Q1-3 PAR2-IgG stimulation resulted in about 1.8-fold and 5.4-fold ($p < 0.05$) activation of ERK1/2 (A) and Akt (B), respectively, when compared to DMEM treated cells (control). However, there was no significant increase of ERK1/2 activation and only about 2.2-fold activation of Akt in the Q4 group when compared to control (Figure 10A-B).

Furthermore, addition of PAR2 peptide blocker (FSLRLRY-NH₂ trifluoroacetate salt) showed a significant reduction of ERK1/2 and Akt activation upon either Q1-3 or Q4 PAR2-IgG stimulation (Figure 10A-B). In conclusion, HMEC-1 treated with Q1-3 PAR2-IgG presented stronger activation of ERK1/2 and Akt when compared with the Q4 group, and that activation could be inhibited by PAR2 peptide blocker.

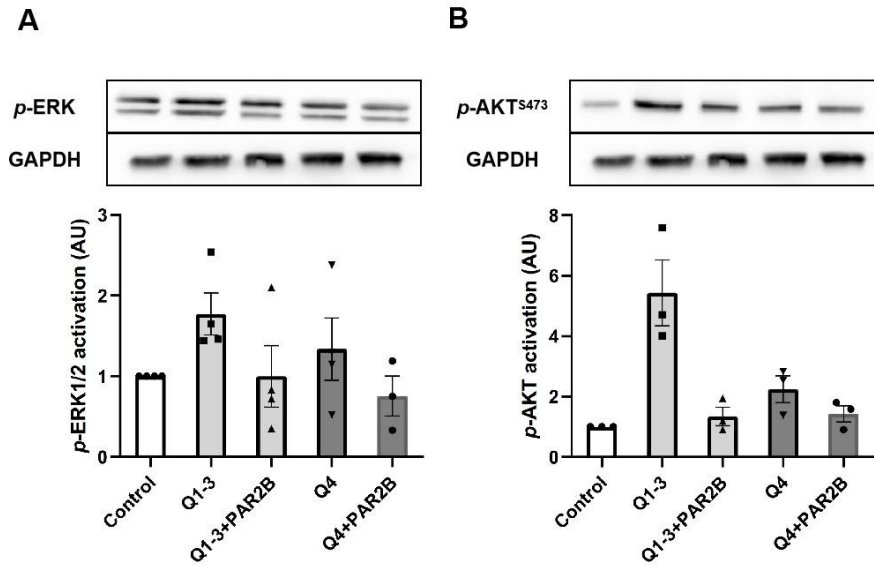


Figure 10. Q1-3 PAR2-IgG induced stronger endothelial ERK1/2 and Akt activation via PAR2. HMEC-1 were pre-incubated for 1 hour with PAR2 peptide blocker (PAR2B) (100nM), and then the effects of Q1-3- or Q4-PAR2-IgG (1mg/mL) on endothelial induction of (A) ERK1/2 and (B) Akt activation were assessed after 15 minutes of stimulation with the indicated IgGs. Values are presented as individual data points together with bars with mean \pm SEM.

4.2.4 Function of PAR2 extracellular loops in G-protein activation in HMEC-1

Analogously to all GPCRs, 3 extracellular loops (ECLs) of PAR2 are potential binding sites of extracellular ligands. Amino acids of individual PAR2 ECL were mutated to alanine constructs named PAR2 ECL1-Ala, PAR2 ECL2-Ala, and PAR2 ECL3-Ala. Our laboratory has optimized these plasmids for G-protein activation [78]. $G_{q/11}$ activation was found to be inhibited by mutation of any ECL, while ERK1/2 activation was inhibited by ECL1 and ECL2 mutation upon trypsin stimulation [78]. The role of ECLs in intracellular signal transduction induced by PAR2-IgG from stroke patients remained unknown. According to the results depicted in Figure 8, the focus was set on $G_{q/11}$ and ERK/2 activation for PAR2-IgG.

Thus, the NFAT and SRE reporter assays were performed to monitor the $G_{q/11}$ and ERK1/2 activation by PAR2-IgG in HMEC-1 over-expressing the wild-type or mutant PAR2.

4.2.4.1 Role of PAR2 ECLs in endothelial $G_{q/11}$ activation induced by PAR2-IgG

Upon Q1-3 PAR2-IgG stimulation, PAR2 wild-type (WT) led to significant activation of $G_{q/11}$ ($p < 0.001$). $G_{q/11}$ activation was also observed in all PAR2 mutants and it showed no obvious alterations when compared to the WT group (Figure 11). Furthermore, there was no significant $G_{q/11}$ constitutive activation due to mutation of ECL1, ECL2, or ECL3, respectively, without stimulation (Figure 11).

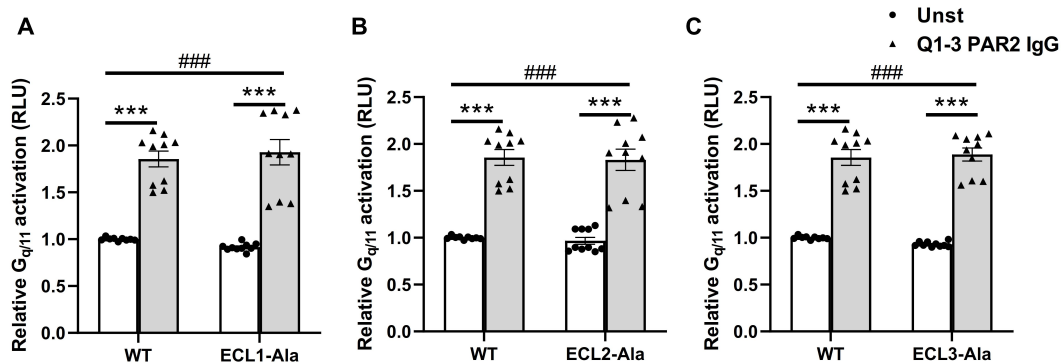


Figure 11. Q1-3 PAR2-IgG-activated $G_{q/11}$ in wild-type or mutated ECLs of PAR2-expressing HMEC-1. (A to C, respectively) HMEC-1 were transfected with WT-PAR2 or different Alanin mutants of ECL1 to 3, and the effects of Q1-3 PAR2-IgG (1mg/mL) on $G_{q/11}$ activation were assessed after 6 hours. *** $p < 0.001$ compares to the unstimulated group in the same PAR2 genotype. ### $p < 0.001$ compares between genotypes. $n = 10$. Values are presented as individual data points together with bars with mean \pm SEM.

By contrast, upon Q4 PAR2-IgG stimulation, PAR2 WT showed no significant activation of $G_{q/11}$ (Figure 12). However, ECL1-Ala presented increased $G_{q/11}$ activation compared to the unstimulated group for either ECL1-Ala ($p < 0.01$) or WT ($p < 0.05$) genotypes (Figure 12A). Furthermore, ECL2-Ala had no $G_{q/11}$ activation compared to WT or unstimulated cells (Figure 12B). Interestingly, upon Q4 stimulation, ECL3-Ala resulted in a significant activation of $G_{q/11}$ compared with WT

genotype ($p<0.001$), unstimulated WT ($p<0.001$), and unstimulated ECL3-Ala ($p<0.001$) (Figure 12C).

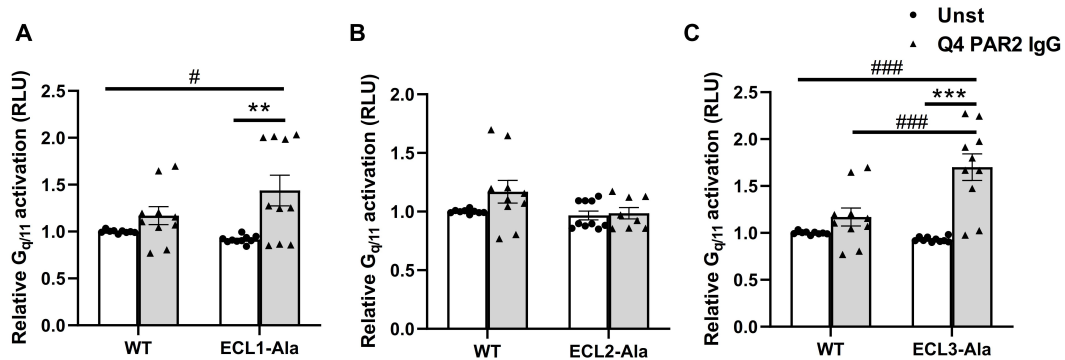


Figure 12. Q4 PAR2-IgG-activated $G_{q/11}$ in wild-type or mutated ECLs of PAR2-expressing HMEC-1. HMEC-1 were transfected with WT-PAR2 or different Alanin mutants of (A) ECL1, (B) ECL2, (C) ECL3, and the effects of Q4 PAR2-IgG (1mg/mL) on $G_{q/11}$ activation were assessed after 6 hours. ** $p<0.01$, *** $p<0.001$ compare to the unstimulated group in the same PAR2 genotype. # $p<0.05$, ### $p<0.001$ compare between genotypes. $n=10$. Values are presented as individual data points together with bars with mean \pm SEM.

4.2.4.2 Role of PAR2 ECLs in endothelial ERK1/2 activation induced by PAR2-IgG

Upon Q1-3 PAR2-IgG stimulation, PAR2 WT led to significant ERK1/2 activation ($p<0.001$). PAR2 mutants also induced ERK1/2 activation and showed no obvious alterations when compared to the WT group with stimulation (Figure 13). However, in absence of stimulation, ECL3-Ala reduced ERK1/2 activation significantly when compared with WT genotype, implying a constitutive inhibition of activation ($p<0.05$) (Figure 13C).

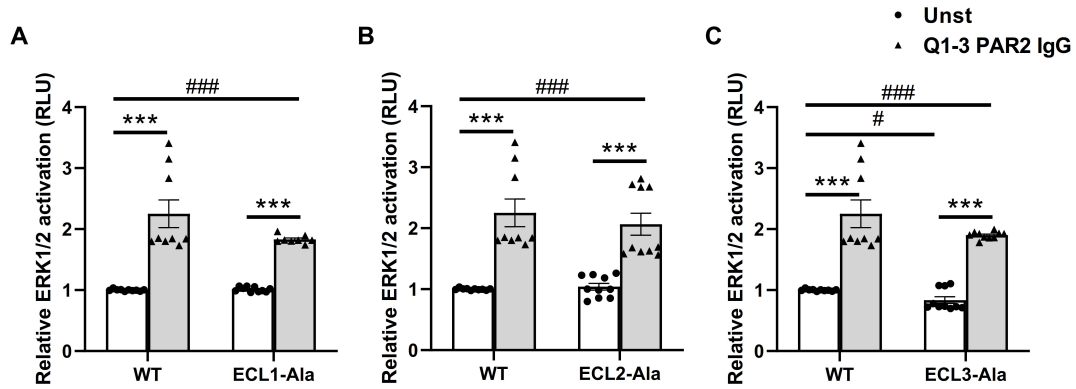


Figure 13. Q1-3 PAR2-IgG-activated ERK1/2 in wild-type or mutated ECLs of PAR2-expressing HMEC-1. (A to C, respectively) HMEC-1 were transfected with WT-PAR2 or different Alanin mutants of ECL1 to 3, and the effects of Q1-3 PAR2-IgG (1mg/mL) on ERK1/2 activation were assessed after 6 hours. *** $p < 0.001$ compares to the unstimulated group in the same PAR2 genotype. # $p < 0.05$ ### $p < 0.001$ compares between genotypes. n=10. Values are presented as individual data points together with bars with mean \pm SEM.

Meanwhile, there was also significant ERK1/2 activation in the WT genotype upon Q4 PAR2-IgG stimulation ($p < 0.001$). Simultaneously, ECL1-Ala ($p < 0.05$) and ECL2-Ala ($p < 0.001$) showed similar effects on ERK1/2 activation when compared with unstimulated control (Figure 14A-B). Notably, ERK1/2 activation showed a significant up-regulation in ECL3-Ala cells when compared to wild-type upon Q4 PAR2-IgG stimulation ($p < 0.001$) (Figure 14C).

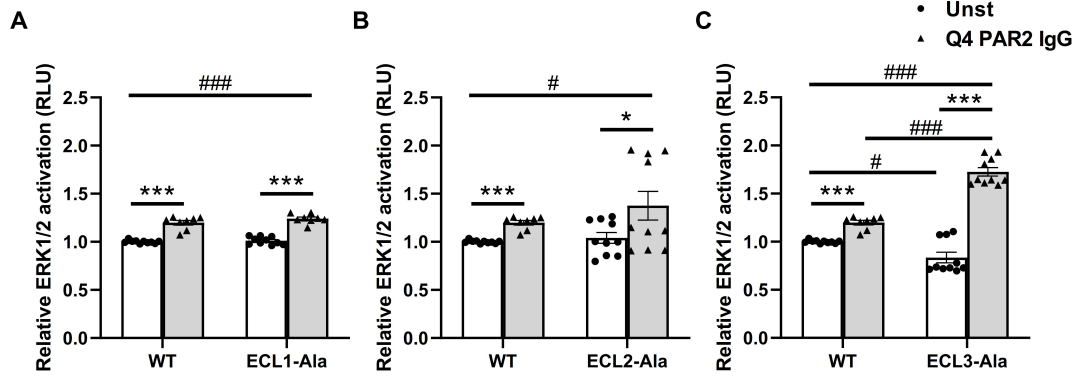


Figure 14. Q4 PAR2-IgG-activated ERK1/2 in wild-type or mutated ECLs of PAR2-expressing HMEC-1. (A to C, respectively) HMEC-1 were transfected with WT-PAR2 or different Alanin mutants of ECL1 to 3, and the effects of Q4 PAR2-IgG (1mg/mL) on ERK1/2 activation were assessed after 6 hours. * $p < 0.05$, *** $p < 0.001$ compare to the unstimulated group in the same PAR2 genotype. # $p < 0.05$, ### $p < 0.001$ compare between genotypes. $n = 10$. Values are presented as individual data points together with bars with mean \pm SEM.

In summary, Q1-3 PAR2-IgG presented a higher level of $G_{q/11}$ and ERK1/2 activation when compared to Q4 PAR2-IgG. Upon Q1-3 stimulation, the $G_{q/11}$ and ERK1/2 activation were not affected by the mutation of extracellular loops. Concerning Q4 PAR2-IgG, the ECL3-Ala mutant produced a Q4 PAR2-IgG-dependent enhanced effect on both $G_{q/11}$ and ERK1/2 activation when compared to wild-type.

4.2.5 Trypsin and PAR2-IgG induced PAR2 internalization in HMEC-1

Receptor internalization is essential for receptor signal transduction, receptor desensitization and endocytosis [83]. Therefore, it was of great interest whether trypsin and PAR2-IgG were able to regulate the surface localization of PAR2.

NanoGlo signal, produced by the HiBiT tag following the Nano-GLO[®]HiBiT Extracellular Detection system, reflects the presence of HiBiT-tagged receptor on the cell membrane. Decreased signal reflects the relative proportion of receptor internalization when compared to the control group [84]. Hence, HiBiT tag was

introduced into the SLIGKV⁴²↓D⁴³GTSHV of the PAR2 receptor in order to measure its membrane expression and internalization.

As shown in Figure 15, trypsin induced a significant reduction of PAR2 membrane expression, indicating that the receptor was internalized in response to the ligand binding. Stimulation with Q1-3 PAR2-IgG also triggered PAR2 internalization, which was much less when compared to trypsin, but still significantly more than Q4 PAR2-IgG ($p<0.01$) (Figure 15).

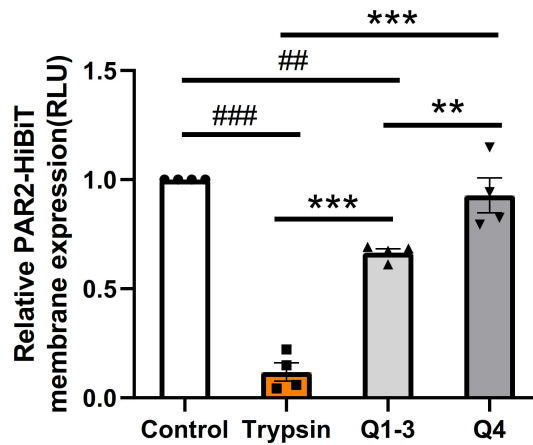


Figure 15. PAR2 expression at the plasma membrane. HMEC-1 were transfected with WT-PAR2-HiBiT plasmid and the effects of trypsin (100nM, stimulation of 20 minutes) or Q1-3- or Q4-PAR2-IgG (1mg/mL, stimulation for 6 hours) on the HiBiT signal were assessed. ** $p<0.01$, *** $p<0.001$ compare between treated groups; ## $p<0.01$, ### $p<0.001$ compare to control group, $n=4$. Values are presented as individual data points together with bars with mean \pm SEM.

4.3 Role of PAR2 in PAR2-IgG-induced G-protein and ERK1/2 activations

As previously shown, $G_{q/11}$, ERK1/2, Akt signaling and PAR2 receptor internalization were promoted by trypsin and Q1-3 PAR2-IgG. To further investigate the effects of PAR2 activation on G-protein activation and intracellular signals including the ERK1/2 pathway, and the effects of the PAR2-ERK1/2 axis on angiogenic genes production, PAR2 peptide blocker (FSLRLRY-NH₂ trifluoroacetate salt) and ERK1/2

blocker (PD 184352) were used.

4.3.1 PAR2 mediates Q1-3 PAR2-IgG-induced $G_{q/11}$ and ERK1/2 activations

Upon Q1-3 PAR2-IgG stimulation, administration of PAR2 peptide blocker partially, but significantly blocked $G_{q/11}$ and ERK1/2 activation with a 24.8% and 51.7% reduction in luciferase activity compared to the Q1-3 group without inhibition (Figure 16A and B). The addition of PAR2 blocker also had a limited inhibitory effect on $G_{q/11}$ and ERK activation after stimulation with Q4-PAR2-IgG (Figure 16A and B).

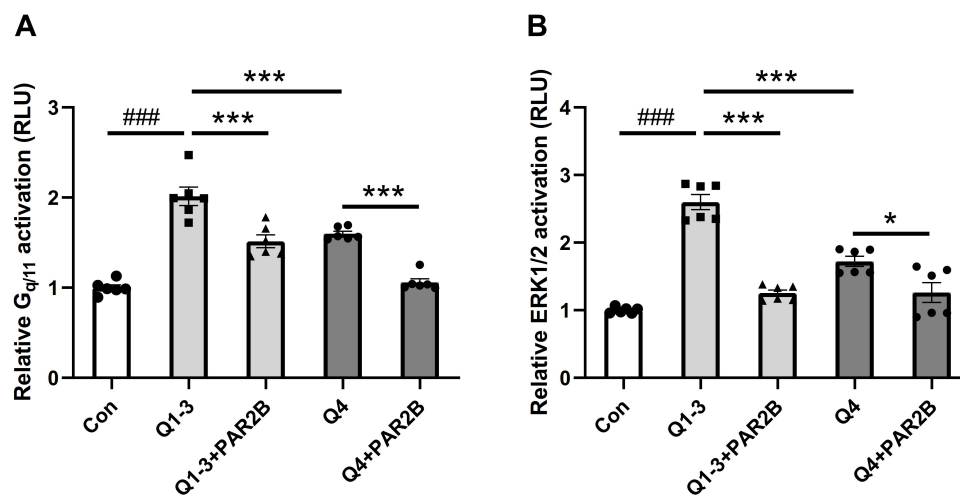


Figure 16. PAR2 inhibition reduced $G_{q/11}$ and ERK1/2 activation by PAR2-IgG in HMEC-1. HMEC-1 were pre-incubated for 1 hour with PAR2 peptide blocker (FSLRLRY-NH2 trifluoroacetate salt, 100nM) and then the effects of Q1-3- or Q4-PAR2-IgG (1mg/mL) on endothelial (A) $G_{q/11}$ and (B) ERK1/2 activation were assessed after 6 hours. * p <0.05, *** p <0.001 compare between treated groups; ### p <0.001 compares to control group, n =6. Values are presented as individual data points together with bars with mean \pm SEM.

4.3.2 Trypsin-induced expression of angiogenic genes and released respective proteins is ERK1/2 dependent

As trypsin regulated ERK1/2 activation, it was investigated if ERK1/2 inhibition influenced the expression of the previously studied angiogenic genes. The results

(Figures 17 and 18) confirmed that ERK1/2 was involved in the regulation of the genes induced by trypsin. ERK1/2 specific blocker decreased dose dependently trypsin induced angiogenic gene transcription. Upon trypsin stimulation, inhibition of ERK1/2 dose-dependently with ERK1/2 specific blocker (PD184352) decreased *VEGF*, *IL-6*, *IL-8*, *CXCL1*, and *ANG2* gene expressions (Figure 17). 10 μ M ERK1/2 blocker demonstrated the most effective suppression, completely blocking the trypsin-induced gene expressions (Figure 17). 0.1 μ M and 1 μ M ERK1/2 blocker had similar inhibitory effects on *VEGF* and *IL-6* genes (Figure 17A-B). The concentration of 0.1 μ M had slight inhibitory effects for all genes except for *ANG2* (Figure 17C).

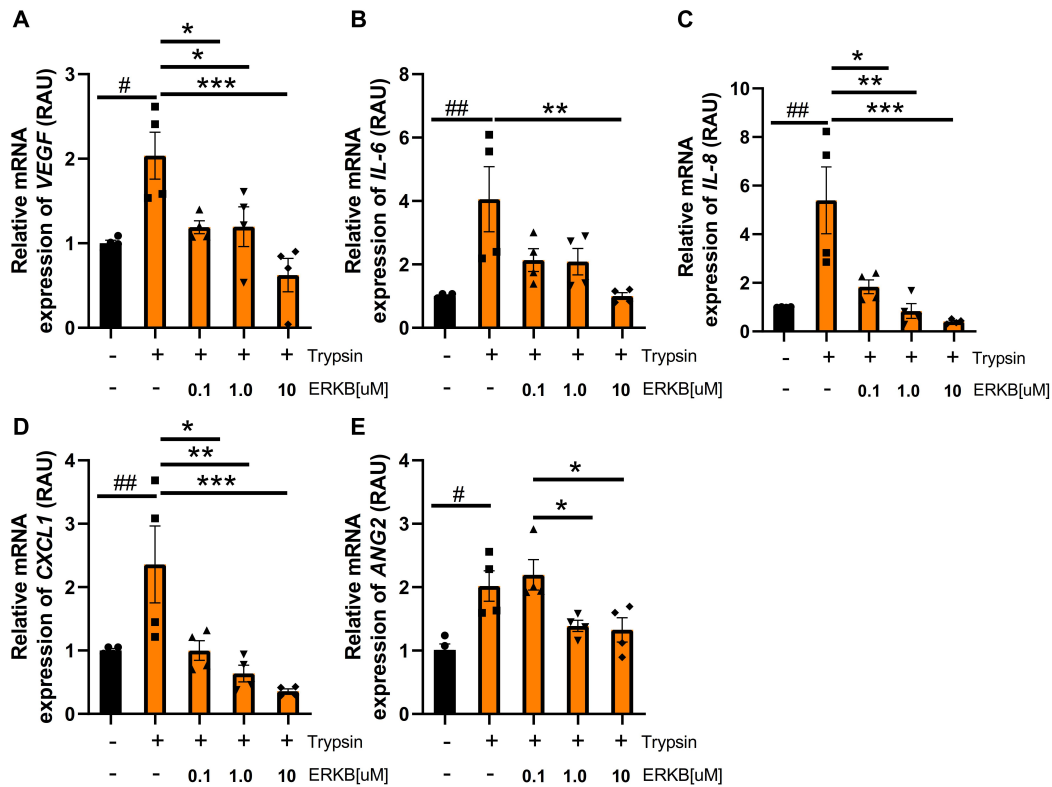


Figure 17. Trypsin-induced expression of angiogenic genes is ERK1/2-dependent. HMEC-1 were pre-incubated for 1 hour with different concentrations of ERK1/2 specific blocker (PD184352, ERKB) (0.1 μ M, 1.0 μ M, 10 μ M) and the effects of trypsin on endothelial proangiogenic gene expressions including (A) *VEGF*, (B) *IL-6*, (C) *IL-8*, and (D) *CXCL1*, were assessed after 1 hour, or for (E) *ANG2* after 6 hours * p <0.05, ** p <0.01, *** p <0.001 compare between treated groups; # p <0.05 ## p <0.01 compares to control group, n=4. Values are presented as individual data points together with bars with mean \pm SEM.

We performed further analysis of cytokine release by ELISA. Consistently with the results depicted in Figure 17, ERK1/2 inhibition decreased the cytokine release in a concentration-dependent manner (Figure 18). There was an approximately 18% reduction of *VEGF* release when treated with 10 μ M ERK1/2 blocker when compared to trypsin stimulation alone ($p<0.05$). There were already statistically significant reductions of *IL-6*, *IL-8*, *CXCL1*, and *ANG2* cytokine releases at ERK1/2 blocker concentrations of 1 μ M ($p<0.01$) or 10 μ M ($p<0.001$). However, 0.1 μ M ERK1/2 blocker only presented significant inhibition of trypsin-induced *ANG2* cytokine release ($P<0.001$).

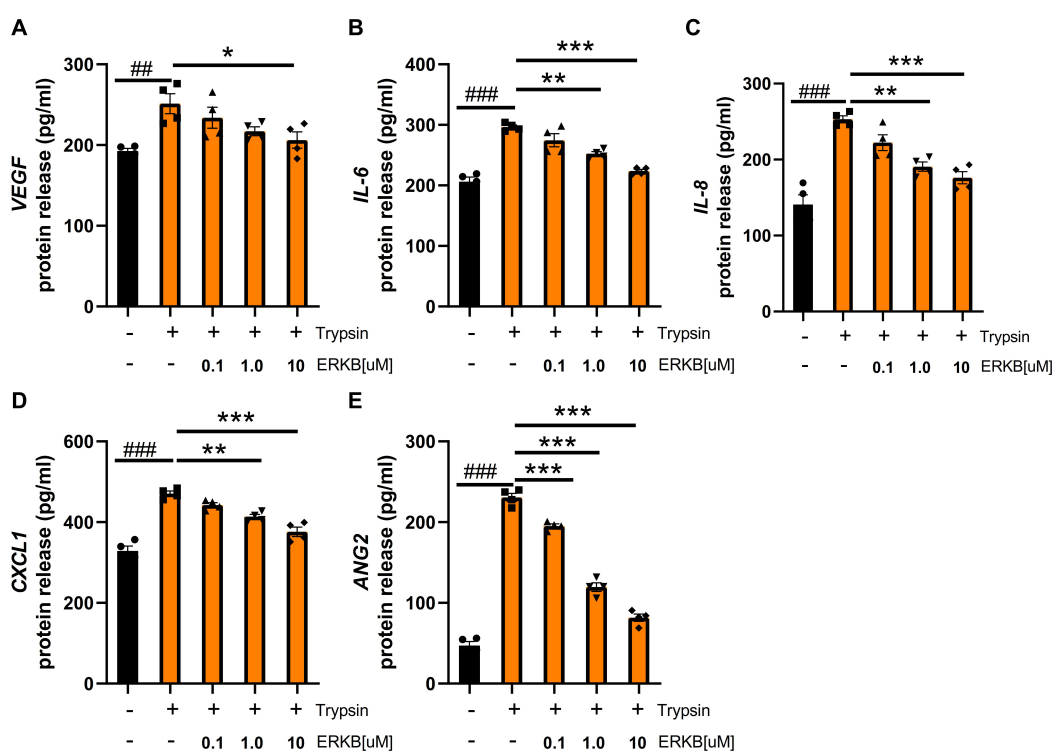


Figure 18. Trypsin-induced release of angiogenic cytokines is ERK1/2-dependent. HMEC-1 were pre-incubated for 1 hour with different concentrations of ERK1/2 specific blocker (PD184352, ERKB) (0.1 μ M, 1.0 μ M, 10 μ M) and the effects of trypsin on endothelial proangiogenic cytokine release including (A) *VEGF*, (B) *IL-6*, (C) *IL-8*, (D) *CXCL1*, and (E) *ANG2* were assessed after 6 hours. * $p<0.05$, ** $p<0.01$, *** $p<0.001$ compare between treated groups; ### $p<0.01$, #### $p<0.001$ compare to control group, n=4. Values are presented as individual data points together with bars with mean \pm SEM.

In conclusion, angiogenic gene expressions and their respective protein secretions were inhibited by ERK1/2 blocker in a concentration-dependent manner, and most effectively with 10 μ M, which was hence used in the following experiments.

4.3.3 Involvement of PAR2 and ERK1/2 signaling in the regulation of angiogenic genes and protein releases by PAR2-IgG

As described previously, trypsin induced the production and secretion of angiogenic cytokines through ERK1/2 signaling. Thus, the effects of ERK1/2 and additionally PAR2 blockers were further investigated on angiogenic gene expressions and protein secretions induced by PAR2-IgG.

4.3.3.1 Effects of PAR2 and ERK1/2 blockers on PAR2-IgG-induced angiogenic gene expressions

As shown in Figure 19, Q1-3 PAR2-IgG significantly increased mRNA levels of (A) *VEGF*, (B) *IL-6*, (C) *IL-8*, and (D) *CXCL1* when compared with those in unstimulated and Q4 PAR2-IgG stimulated endothelial cells. Notably, Q1-3 and Q4 promoted the mRNA production of *ANG2* when compared with the unstimulated group ($p < 0.001$) (Figure 19E).

In addition, administration of PAR2 and ERK1/2 blockers completely inhibited *VEGF* mRNA expression (Figure 19A), and partially blocked the mRNA expression of *IL-6*, *IL-8*, and *CXCL1* upon Q1-3 PAR2-IgG (Figure 19B-D). This demonstrated that PAR2-IgG-induced mRNA expression of *VEGF* was completely mediated by PAR2 whereas for the other cytokines alternate signaling pathways might have contributed to their increased gene expression in response to PAR2-IgG.

Upon Q4 PAR2-IgG stimulation, there were no significant alterations of *VEGF*, *IL-6*, *IL-8* and *CXCL1* mRNA levels, as well as no effects of cell pretreatments with PAR2 or ERK1/2 blockers.

Interestingly, ERK1/2 blocker presented stronger inhibitory effects on *CXCL1* and *ANG2* transcription than PAR2 blocker in response to Q1-3- or Q4-PAR2-IgG stimulation. This suggested that Q1-3- or Q4-PAR2-IgG induced *ANG2* expressions

by ERK1/2, but not solely by PAR2. Alternative ERK1/2 upstream signaling pathways might contribute to PAR2-IgG-induced *ANG2* expressions.

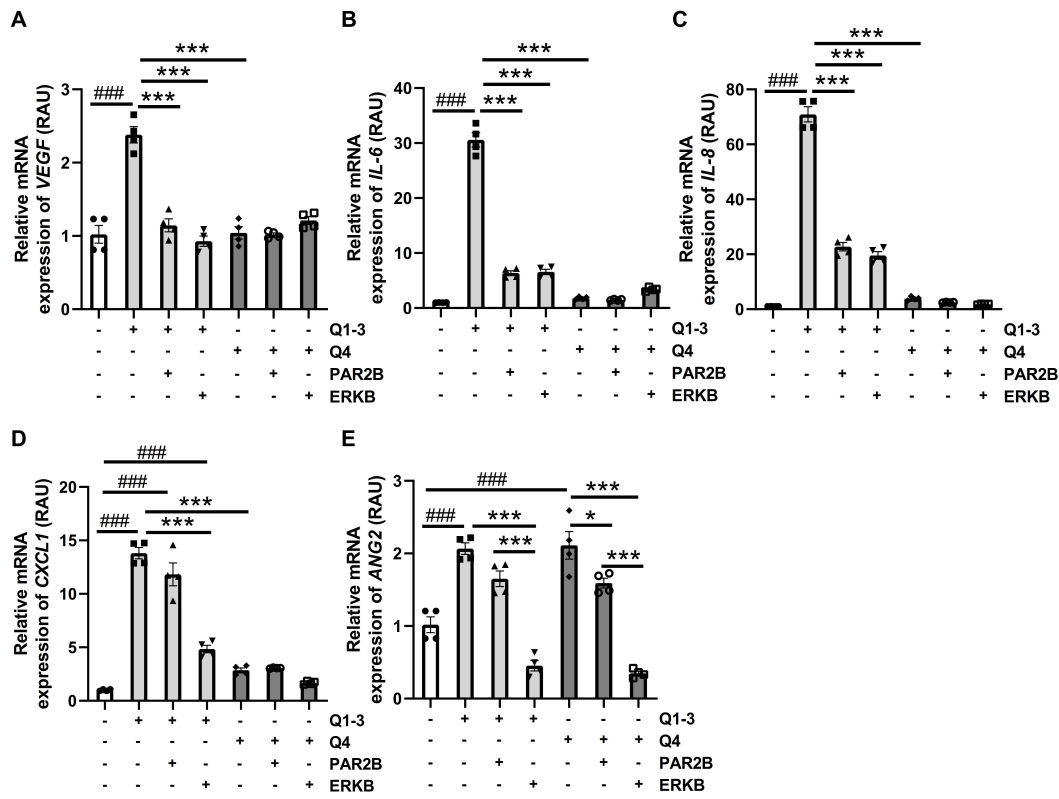


Figure 19. PAR2- and ERK1/2-dependence of PAR2-IgG induced expressions of endothelial angiogenic genes. HMEC-1 were pre-incubated for 1 hour either with PAR2 peptide blocker (FSLRLRY-NH2 trifluoroacetate salt, PAR2B) (100nM) or ERK1/2 specific blocker (PD184352, ERKB) (10 μ M) and then the effects of Q1-3 or Q4-PAR2-IgG (1mg/mL) on endothelial proangiogenic gene expressions including (A) *VEGF*, (B) *IL-6*, (C) *IL-8*, and (D) *CXCL1* were assessed after 1 or (E) *ANG2* after 6 hours. * p <0.05, *** p <0.001 compare between treated groups; ### p <0.001 compares to control group, n=4. Values are presented as individual data points together with bars with mean \pm SEM.

4.3.3.2 Effects of PAR2 or ERK1/2 blockers on PAR2-IgG-induced angiogenic cytokine secretions

Next, the cytokine secretions were assessed. As shown in the Figure 20, Q1-3 PAR2-IgG contributed to about 2.4-, 2.9-, 2.7-, and 2.2-fold increase in protein release of (A) *VEGF*, (B) *IL-6*, (C) *IL-8*, and (D) *CXCL1*, respectively (p <0.001), while there were also significant protein releases of VEGF (about 1.6 fold, p <0.05) and CXCL1

(about 1.6 fold, $p < 0.001$) when stimulated with Q4 PAR2-IgG compared to the control group. Q1-3 PAR2-IgG presented higher activation of the above-mentioned protein releases than those in the Q4 group (Figure 20A-D, $p < 0.05$).

Q1-3 and Q4 PAR2-IgG promoted a similar protein release of ANG2 (E) when compared to control group ($p < 0.001$).

Moreover, administration of PAR2 peptide blocker or ERK1/2 blocker partially inhibited the protein release of all the angiogenesis cytokines induced by Q1-3 PAR2-IgG. ERK1/2 blocker demonstrated the most effective inhibition. This implied that alternative ERK1/2 upstream signaling pathways might contribute to the angiogenic cytokine release induced by Q1-3 PAR2-IgG.

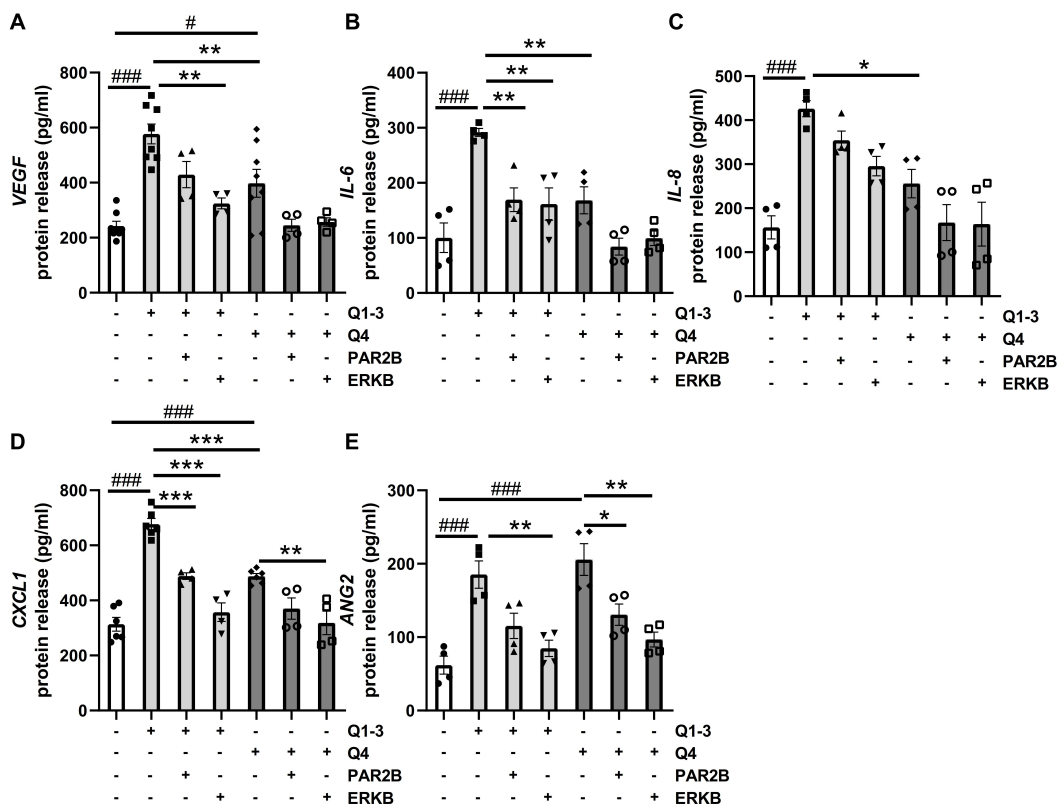


Figure 20. PAR2-IgG induces endothelial angiogenic cytokine release via PAR2 and ERK1/2 signaling. HMEC-1 were pre-incubated for 1h either with PAR2 peptide blocker (FSLRLRY-NH2 trifluoroacetate salt, PAR2B) (100nM) or ERK1/2 specific blocker (PD184352, ERKB) (10 μ M), and then the effects of Q1-3- or Q4-PAR2-IgG (1mg/ml) on endothelial angiogenic cytokines release including (A) *VEGF*, (B) *IL-6*, (C) *IL-8*, (D) *CXCL1*, and (E) *ANG2* were assessed after 6 hours.

* $p < 0.05$, ** $p < 0.01$, *** $p < 0.001$ compare between treated groups; # $p < 0.05$, ### $p < 0.001$ compare to control group, $n \geq 4$. Values are presented as individual data points together with bars with mean \pm SEM. In conclusion, PAR2-IgG and trypsin regulated angiogenic gene transcription and protein release through the PAR2-ERK1/2 signaling pathway. Notably, Q1-3 PAR2-IgG presented a much higher activation of pro-angiogenic gene expressions than Q4 PAR2-IgG.

4.4 Regulatory mechanism of trypsin and PAR2-IgG-induced VEGF transcription

4.4.1 Detection of transcription factor binding sites regulating VEGF promoter activity induced by trypsin and PAR2-IgG

As shown previously, VEGF could be regulated by trypsin and Q1-3 PAR2-IgG at the transcription level. To investigate potential sequences on the *VEGF* promoter, which might respond to trypsin and PAR2-IgG in HMEC-1, different truncations of *VEGF* promoter were used.

As shown in Figure 21, the deletion of the *VEGF* promoter sequence between -2068 to -1340bp led to a slight reduction of *VEGF* promoter activation, while deleting the *VEGF* promoter sequence between -1339 to -839 bp led to significant reduced activation of *VEGF* upon trypsin (Figure 21A) and Q1-3 PAR2-IgG (Figure 21B) stimulation.

Notably, it has been reported that two AP-1 binding sites locating at the -1227 to -1215 bp and -937 to -925 bp regions of the *VEGF* promoter responded to hyperbaric oxygen in human umbilical vein endothelial cells [37]. Therefore, the response sequences locating on the *VEGF* promoter sequence from -1339 to -839 were most likely to be AP-1 binding sites. Therefore, AP-1 inhibitor was used to verify the effects of AP-1 on *VEGF* promoter activation.

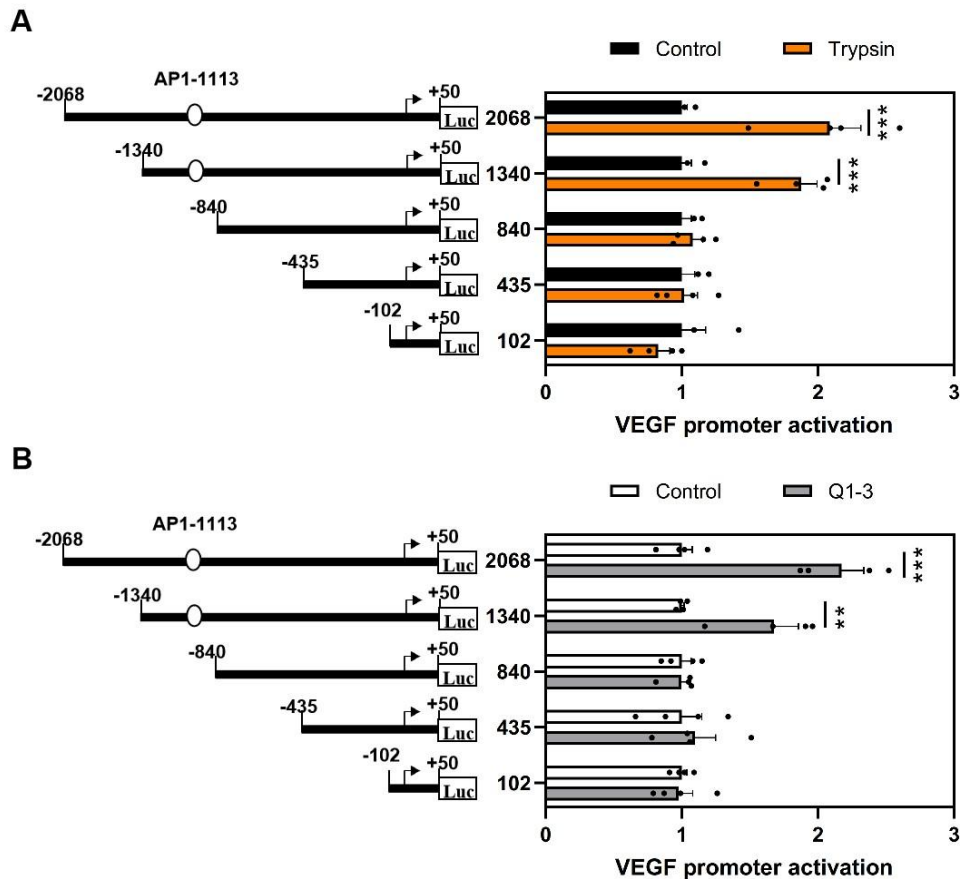


Figure 21. Detection of transcription factor binding sites regulating VEGF promoter activity induced by trypsin and PAR2-IgG. HMEC-1 were transiently transfected with full length (2068) or truncated *VEGF* promoter constructs and stimulated with 100nM trypsin (A) or Q1-3 PAR2-IgG (1mg/mL) (B) for 6 hours. Luciferase activity was determined and expressed as relative light units (RLU). ** $p < 0.01$, *** $p < 0.001$ compare to control with same promoter construct, $n = 4$. Values are presented as individual data points together with bars with mean \pm SEM.

4.4.2 Involvement of AP-1 in *VEGF* promoter activation in HMEC-1

Transcriptional regulatory mechanisms leading to *VEGF* induction are complex. AP-1 has been shown to be involved in *VEGF* induction, thereby promoting angiogenesis [37, 85]. ERK1/2 is involved in a plethora of transcriptional mechanisms including the regulation of AP-1, which in turn promoted *VEGF* transcription [37]. Therefore, the role of AP-1 in the transcription of *VEGF* following PAR2 activation by trypsin and PAR2-IgG was investigated using an AP-1 inhibitor. As shown in Figure 22, the

transcription of *VEGF* was significantly reduced when compared to the control when cells stimulated with trypsin and Q1-3 PAR2-IgG were under AP-1 inhibition. This implied that AP-1 was involved in the VEGF promoter activation induced by trypsin and Q1-3 PAR2-IgG.

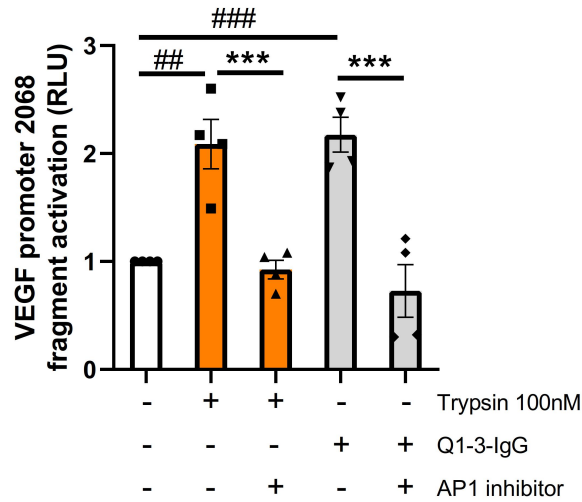


Figure 22. Effect of AP-1 inhibitor on human *VEGF* promoter in response to trypsin and PAR2-IgG. HMEC-1 were transiently transfected with *VEGF* promoter 2068 construct and pre-incubated for 1 hour with AP-1 inhibitor (100 nM) before stimulation with 100nM trypsin or Q1-3 PAR2-IgG (1mg/mL) for 6 hours. Luciferase activity was determined and expressed as relative light units (RLU). *** $p < 0.001$ compares between treated groups; ### $p < 0.001$ compares to control group, $n = 4$. Values are presented as individual data points together with bars with mean \pm SEM.

4.5 PAR2/ERK1/2 signaling were involved in PAR2-IgG-induced endothelial angiogenesis

Cells treated with PAR2 or ERK blocker showed a obvious reduction in the release of pro-angiogenic cytokines upon activation of either Q1-3 PAR2-IgG or Q4 PAR2-IgG. However, the involvement of PAR2 and ERK1/2 in the IgG-induced angiogenesis regulation was unknown. As demonstrated in Figure 23A, PAR2 peptide blocker significantly reduced the vascular tube formation induced by Q1-3 PAR2-IgG. Furthermore, ERK1/2 specific blocker presented a more potent inhibitory effect on

vascular tube formation upon either Q1-3 or Q4 PAR2-IgG (Figure 23A and B).

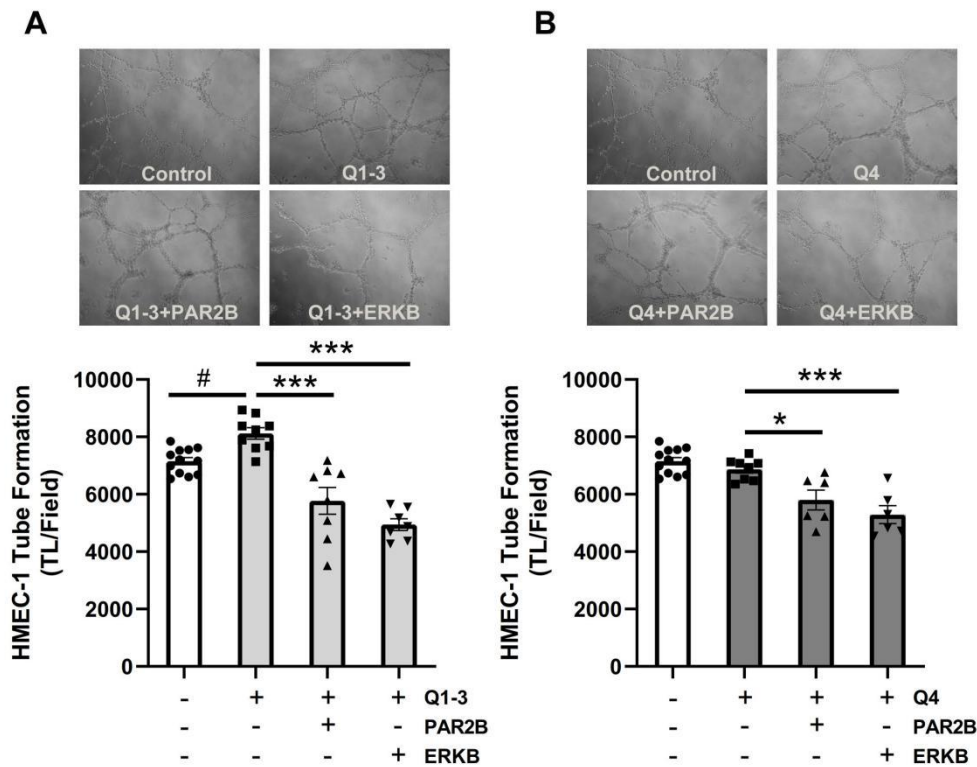


Figure 23. PAR2-IgG regulated endothelial cell tube formation via PAR2/ERK1/2 signaling pathway. HMEC-1 were pre-incubated for 1 hour with specific blockers (PAR2 peptide blocker and ERK1/2 specific blocker) and then the effect of (A) Q1-3- or (B) Q4-PAR2-IgG (1mg/mL) on endothelial cell tube formation was assessed after 16 hours. $**p<0.01$, $***p<0.001$ compare between treated groups; $###p<0.001$ compares to control group. Values are presented as individual data points together with bars with mean \pm SEM. Representative phase contrast images (magnification 100X) are demonstrated in order corresponding to the experimental groups depicted in the graph at the bottom.

4.6 Effect of PAR2-IgG on angiogenesis in brain microvascular endothelial cells

The above results demonstrated that PAR2 activation induced by trypsin and PAR2-IgG promoted angiogenesis through the ERK1/2 pathway in HMEC-1. However, HMEC-1 are not a physiological model for stroke. Thus, the effect of PAR2-IgG on tube formation was additionally assessed in brain microvascular endothelial cells (hCMEC/D3). As shown in Figure 24, Q1-3 PAR2-IgG presented

enhanced capacities of tube formation when compared with unstimulated or with Q4 PAR2-IgG-stimulated cells. Consistently with the angiogenesis function in HMEC-1, these results confirmed that PAR2-IgG are physiologically relevant in brain endothelial cells.

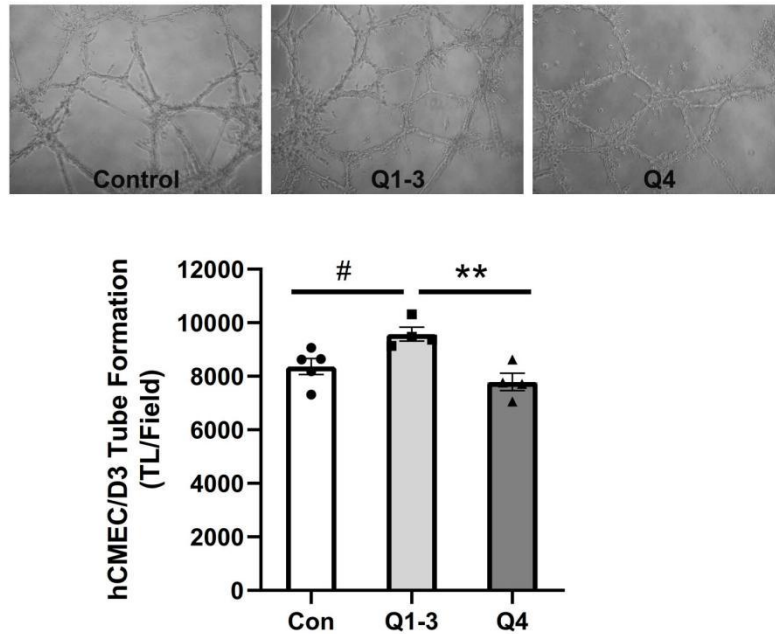


Figure 24. Effect of PAR2-IgG on hCMEC/D3 tube formation. Cells were stimulated with IgG isolated from the plasma of stroke patients with Q1-3 or Q4-PAR2-IgG (1mg/mL). Endothelial cell tube formation was assessed after 16 hours. Representative phase-contrast images (magnification 100X) are presented in the upper panel. Below, quantifications of the tube formations under the different conditions as indicated are shown. Values are presented as individual data points together with bars with mean \pm SEM. ** $p < 0.01$ compares between treated groups; # $p < 0.05$ compares to control group, $n = 4$.

5. Discussion

In the management of acute ischemic stroke, rapid recovery by the re-establishment of blood flow is the preferred therapeutic strategy. Several studies have found that angiogenesis and its enhancement are relevant in the pathophysiology and recovery process of cerebral ischemia [7, 10].

A doctoral thesis demonstrated that PAR2-IgG isolated from kidney transplant patients showed a reduced effect on VEGF expression compared to healthy individuals [77]. Intriguingly, unpublished clinical data from the group leader PD. Dr. Thomas G. Liman demonstrated that patients with PAR2-IgG levels in the top quartile were at increased risk of poor outcome one year after stroke onset. However, the functions and mechanisms of PAR2-IgG in ischemic stroke remain unclear.

In this study, the G-protein activation and regulatory mechanisms of VEGF release in angiogenesis induced by trypsin and PAR2-IgG were investigated. The results demonstrated that the PAR2 natural agonist trypsin generated the activation of different G-protein subunits and ERK1/2 pathway mediating angiogenic gene expression. Importantly, low level PAR2-Ab (Q1-3 PAR2-IgG) triggered the G_{q/11} and intracellular ERK1/2 signaling pathways leading to enhanced protein release and transcription of VEGF, IL-6, IL-8, CXCL1 when compared to the highest level PAR2-Ab (Q4 PAR2-IgG). These effects were inhibited by PAR2 and ERK1/2 specific blockers. In addition, the activation of the *VEGF* promoter by PAR2-IgG was down-regulated by AP-1 inhibition. Effective response sequences on the *VEGF* promoter might be located in the -1339 to -839 bp region. Furthermore, endothelial angiogenesis in HMEC-1 and hCMEC/D3 cells was up-regulated by PAR2-IgG in Q1-3 individuals when compared to that in Q4 individuals. Thus, PAR2-IgG in Q1-3 presented pro-angiogenic activities and agonistic function *in vitro*. However, the complexity of Q4 PAR2-IgG needs to be further verified.

5.1 Characteristics of PAR2-IgG isolated from stroke

patients

As previously mentioned, PAR2-IgG isolated from the plasma of stroke patients was classified into Q1-3 (<14 unit/mL) and Q4 (>14 unit/mL); Q4 patients had a poor outcome after being adjusted by age, sex, etiological subtypes, stroke severity, pre-stroke dependency, and vascular risk factors. Our preliminary results demonstrated that the Q1-3 PAR2-IgG with stimulating effects showed more PAR2 internalization, G-protein signal activation, production of angiogenic factors and enhanced new vessel formation than those in the Q4 PAR2-IgG with weak stimulating or neutral effects.

In recent years, studies have provided evidence that autoantibodies function differently, for example, the classical TSH receptor autoantibodies with different functional capabilities (stimulating, blocking, and cleavage) have been verified in Graves' disease [86, 87]. In addition, IgG subclasses (with different functions) are normally named in descending order of frequency, e.g., IgG1, IgG2, IgG3, and IgG4 [88]. Normally, IgG4 accounts for 5% of total IgG in human plasma [88]. IgG4 seems to prevent the harmful effects (e.g., inflammatory response) of other antibody subclasses by competition for antigen to block the binding of other IgG subclasses without exerting an effector function [89, 90]. In this study, Q4 with higher titer PAR2-IgG demonstrated a more inefficient G-protein activation than Q1-3 PAR2-IgG with lower titer, which might be due to the presence of more blocking antibodies in PAR2-IgG in Q4. Furthermore, based on the severity of the stroke, the functions, and subclasses of PAR2-IgG might be not completely the same in the Q1-3 and Q4 groups. In addition, it has been reported that autoantibodies against oxidized low-density lipoprotein could contribute to a cascade of events characterized as immunoinflammatory reactions of ischemic stroke [91]. There might be other IgGs co-isolated by IgG purification in the Q1-3 and Q4 groups which contribute to the pathological functions in stroke despite PAR2 specific blocker having been used to test the specificity of PAR2 signaling. Therefore, the differences between, and characteristics of Q1-3 and Q4 PAR2-IgG certainly need to be further investigated

based on monoclonal PAR2-IgG in the near future.

5.2 G-protein coupling of PAR2

Luciferase reporter assay was applied to detect G-protein activation induced by trypsin and PAR2-IgG. In this detection system, increased activities of NFAT, SRF, and SRE reflected $G_{q/11}$, $G_{\alpha 12/13}$, and ERK1/2 activation following PAR2 activation [81].

In this case, unlike the G-protein subunits activated by trypsin, PAR2-IgG isolated from stroke patients activated $G_{q/11}$, and ERK1/2 but not $G_{\alpha 12/13}$. One study demonstrated that PAR2 is a typical receptor of $G_{q/11}$ coupling which mediates intracellular calcium via the PLC/IP3 pathway, and $G_{\alpha 12}$ coupling presented kinetics with a very slow and sustained activation by trypsin until about 30 minutes [92]. Another study carried out by Kelly L. McCoy in PAR-null COS7 cells showed that ectopically expressed PAR2 can couple to $G_{q/11}$ family members as well as $G_{\alpha 12/13}$ family members to activate the downstream signaling pathways, but not to G_o and G_i family members by PAR2-activating peptides (APs) [93].

In other contexts, ERK1/2 has been shown to be activated by other G-protein signaling such as $G_{q/11}$, G_s , $G_{\beta\gamma}$, and β -arrestins [94]. $G_{q/11}$ coupling induces production of DAG and PKC, which regulates ERK1/2 activation thorough Raf [55]. Accumulated cAMP generated by G_s activation and inhibited by G_i activation can activate ERK1/2 via the Epac/Rap-1/B-Raf pathway or indirectly via PKA [95]. Additionally, specific modulation of ERK1/2 results from elevated cAMP or PKA activation, while $G_{\beta\gamma}$ subunits released from activating coupled G_s can activate the MAPKs pathway [95]. Endocytosis of PAR2 mediated by β -arrestin leads to cytosolic ERK1/2 activation, which does not translocate to the nucleus. Conversely, a point mutant of PAR2 (δ ST363/6A) is independent of β -arrestin interaction and causes ERK1/2 activation by a Ras-dependent pathway [96]. Prolonged ERK1/2 activation in the status of a scaffolding complex mediated by β -arrestin is required for localized actin assembly and chemotaxis in pseudopodia [97]. It was not possible to include

tests for all possible G-proteins known to activate ERK1/2 within this thesis work. Its additional focus was set to the downstream consequences induced by G_{q11} and ERK1/2 activation initiated signaling cascade.

5.3 PAR2 and VEGF/VEGFR signaling

PAR2 has been involved in angiogenesis via the cross-talk between PAR2 and the VEGF/VEGFR system [77]. The results of this study demonstrated that PAR2 activation induced by trypsin and Q1-3 PAR2-IgG promoted transcription and protein secretion of VEGF via the ERK1/2-AP-1 signaling pathway.

Other researchers have also demonstrated that PAR2 activation triggers a proangiogenic effect by increasing VEGF expression *in vivo* and *in vitro*. A.F. Milia *et al.* reported that injection of PAR2-AP or trypsin enhanced reparative angiogenesis, which resulted in accelerated hemodynamic recovery and limb salvage in mice [69]. PAR2, which is abundantly distributed in retinal ganglion cells, can promote neovascularization through activating the transcription of VEGF promoter via Sp1 during retinal development, as well as ischemic retinopathy [98].

In this study, trypsin or Q1-3 PAR2-IgG stimulation facilitated the activation of ERK1/2 and Akt. Inhibition of PAR2 or ERK1/2 signal decreased the expression of VEGF and angiogenesis *in vitro*. L.H. Chang *et al.* reported that PAR2 activation promoted pancreatic cancer angiogenesis through enhanced VEGF secretion via the ERK1/2 signaling, independently of the ILK/HIFs- α pathways [99]. In human adipose stem cells, the MEK/ERK1/2 and PI3k/Akt pathways are involved in the production and release of VEGF upon trypsin stimulation [100]. However, in glioblastoma (GBM) cell lines, ERK1/2, not the PI3k/Akt pathway induced by PAR2-AP, was able to modulate VEGF production [38]. Thus, the production of VEGF and other angiogenic factors seems to be differently regulated depending on cell type and physiological or pathological context.

Given the fact that trypsin and Q1-3 PAR2-IgG stimulation led to VEGF induction at transcription and translation levels, the VEGF promoter assay was applied to

investigate whether PAR2 activation regulated the promoter activation of VEGF. The specific sequences on the VEGF promoter which respond to trypsin and PAR2-IgG stimulation were explored by taking advantage of different truncations of VEGF promoter fragments. The results showed that response sequences could be located in the *VEGF* promoter sequence from -1339 to -839 bp. It was reported that AP-1 binding sites are located between -1227 to -1215 bp and between -937 to -925 bp, respectively [37]. Subsequently, AP-1 inhibitor was applied and assessed its effects on *VEGF* promoter activation. The specificity of the AP-1 binding site remains to be confirmed by Electrophoretic mobility shift assay (EMSA).

Further ways to regulate VEGF expression have been reported in the literature. In HEK293 cells, PAR2 translocated to the nucleus and facilitated the recruitment of Sp1 to trigger VEGF expression [98]. PAR2 activation induced the production of VEGF via HIF-independent pathways, despite the fact that PAR2 activation altered the protein levels of HIF-1 α and HIF-2 α [99]. In addition, post-transcriptional regulation including mRNA stabilization enriched mRNA expression rather than activating the promoter of genes. A contribution of these mechanisms of VEGF mRNA induction by trypsin or PAR2-IgG should be investigated in further studies.

5.4 PAR2 and angiogenesis signaling

In addition to VEGF release, this thesis work detected that activation of PAR2 induced mRNA and protein release of IL-6, IL-8, and CXCL1 via the ERK1/2 pathway. Several studies have indicated that enhanced secretion of these angiogenic cytokines could lead to VEGF production. IL-6 in synergy with sIL-6R enhanced VEGF production and secretion in human peritoneal mesothelial cells (HPMCs) through STAT3 and SP4 activating the VEGF promoter [101]. The addition of recombinant IL-8 stimulated VEGF production and secretion in non-tumorigenic SBcl2 primary melanoma cells and promoted angiogenesis [102]. It was reported that overexpression of CXCL1 promoted xenograft local gastric tumor growth through increased levels of *p*-STAT3, VEGF, and microvessel density [103]. Thus, a thorough

understanding of the cross-talk between these cytokines and VEGF is of significance upon PAR2 activation by trypsin or PAR2 IgG in endothelial cells.

Notably, in this study, angiogenic factor ANG2 was up-regulated upon PAR2 activation induced by trypsin, Q1-3, and Q4 PAR2-IgG. The role of ANG2 in angiogenesis is mainly involved in destabilizing blood vessels, pathological angiogenesis, enhanced vascular permeability, and vascular inflammation. Several experimental data have found that ANG2 destabilizes blood vessels by counteracting the Ang1-Tie2 signals and interaction within endothelial-periendothelial cells [104]. C. Peter *et al.* reported that ANG2 was a natural antagonist for Tie2 to disrupt angiogenesis *in vivo* [105]. Notably, endothelial ANG2 in synergy with VEGF was reported to promote the sprouting of new vessels, while in the absence of VEGF, new vessels would undergo regression by endothelial cell apoptosis induced by ANG2 [106]. Q1-3 PAR2-IgG promoted endothelial angiogenesis through the production of more of the above-mentioned angiogenic cytokines than those in the Q4 PAR2-IgG group, except for ANG2. Secreted ANG2 in the Q4 group might exhibit inhibitory effects on angiogenesis due to a shortage of VEGF.

However, the regulatory molecular mechanisms of ANG2 activated by Q4 PAR2-IgG remain unclear. In this regard, further exploration of ANG2 as a context-dependent mediator of angiogenesis may be required.

5.5 ECLs and PAR2 activation

In addition to PAR2 downstream signaling, this work investigated the involvement of ECLs in PAR2 activation upon trypsin and PAR2-IgG stimulation. More attention has been paid to the role of ECLs over the past few years, especially after several publications revealed that ECLs are involved in ligand binding.

It was reported that the substitution of six conserved amino acids with alanine in the ECL1 of neurotensin receptor 1 led to a maximal loss of the agonist-specific binding capacity [107]. ECL1 was a critical determinant for CP 55940-induced human cannabinoid receptor 1 activation, which resulted from a loss of affinity for CP 55940

agonist in ECL1 mutation [108]. In this study, mutation of ECL1 of PAR2 to alanine decreased G_{q11} and ERK1/2 activation upon trypsin stimulation, while ECL1 had no significant effects upon PAR2-IgG activation.

ECL2 is the longest loop among all ECLs of PAR2. Previous research regarding AT_1R and $ET_A R$ in our laboratory revealed the significance of ECL2 in ligand binding and receptor activation [109]. B. Al-Ani reported that site-directed mutagenesis of ECL2 in rat PAR2 reduced the potency of trypsin and other agonistic peptides (e.g. SLIGRL-NH₂) on calcium signaling [47].

Within this thesis work, the mutation of ECL2 down-regulated the potency of trypsin on G_{q11} and ERK1/2 activation, while ECL2 displayed no significant effects on PAR2-IgG-induced ERK1/2 and $G_{q/11}$ activation.

Intriguingly, additional results displayed that mutation of ECL3 was able to increase the $G_{q/11}$ and ERK1/2 activation induced by Q4 PAR2-IgG, which implied that ECL3 might be a binding site for antagonistic PAR2 autoantibodies. Simultaneously, the substitution of ECL3, however, had no obvious alterations for $G_{q/11}$ and ERK1/2 activation by trypsin and Q1-3 PAR2-IgG. To date, other studies regarding the functions of ECL3 have been limited. ECL3 mutations of the FSH receptor induced higher receptor internalization by FSH, but simultaneously contributed to impaired phosphorylation of ERK1/2 [110]. Additionally, the ECL3 of noradrenaline transporter contributes to the binding selectivity of substrates and inhibitors [111]. ECLs might play a fundamental role in receptor internalization. In this study, the Q1-3 PAR2-IgG promoted wild-type PAR2 internalization when compared to Q4 PAR2-IgG. Further investigation for ECL-mediated receptor internalization and IgG subclass binding sites will be of extreme importance in the future to regulate receptor functions.

6. Future Prospects

The present work elucidated new PAR2 signaling pathways induced by PAR2-IgG in human endothelial cells (ECs). In brief, Q1-3 PAR2-IgG led to increased receptor

internalization, G-protein activation of PAR2, ERK1/2 activation, and angiogenic gene production, finally leading to up-regulation of angiogenesis. Low PAR2-IgG in the Q1-3 group led to an increase in the pro-angiogenic genes and angiogenesis when compared to the high PAR2-IgG levels of Q4 group. This may offer new therapeutic avenues to ameliorate or even halt stroke progression at an early stage.

Based on the thesis results, the following aspects may need to be explored in the future:

- 1) Purified monoclonal autoantibodies could be purified and used to investigate the potential binding sites on PAR2, its G-protein subunit activation and possible ECL-mediated receptor internalization.
- 2) Furthermore, one could explore whether independent coupling of Gs, Gi, or β -arrestins regulates the activation of ERK1/2 when stimulated with trypsin and PAR2-IgG.
- 3) It is also important to look for the contribution of the PI3k/Akt pathway to the regulation of the ERK pathway, the production of VEGF, and other angiogenic factors.

References

1. Benjamin EJ, Virani SS, Callaway CW, Chamberlain AM, Chang AR, Cheng S, Chiuve SE, Cushman M, Delling FN, Deo R, de Ferranti SD, Ferguson JF, Fornage M, Gillespie C, Isasi CR, Jiménez MC, Jordan LC, Judd SE, Lackland D, Lichtman JH, Lisabeth L, Liu S, Longenecker CT, Lutsey PL, Mackey JS, Matchar DB, Matsushita K, Mussolino ME, Nasir K, O'Flaherty M, Palaniappan LP, Pandey A, Pandey DK, Reeves MJ, Ritchey MD, Rodriguez CJ, Roth GA, Rosamond WD, Sampson UKA, Satou GM, Shah SH, Spartano NL, Tirschwell DL, Tsao CW, Voeks JH, Willey JZ, Wilkins JT, Wu JH, Alger HM, Wong SS, and Muntner P, *Heart Disease and Stroke Statistics-2018 Update: A Report From the American Heart Association*. *Circulation*, 2018. **137**(12): p. e67-e492.
2. Wang SW, Liu Z, and Shi ZS, *Non-Coding RNA in Acute Ischemic Stroke: Mechanisms, Biomarkers and Therapeutic Targets*. *Cell Transplant*, 2018. **27**(12): p. 1763-77.
3. Khandelwal P, Yavagal DR, and Sacco RL, *Acute Ischemic Stroke Intervention*. *J Am Coll Cardiol*, 2016. **67**(22): p. 2631-44.
4. Ciccone A, Valvassori L, Nichelatti M, Sgoifo A, Ponzio M, Sterzi R, Boccardi E, and Investigators SE, *Endovascular treatment for acute ischemic stroke*. *N Engl J Med*, 2013. **368**(10): p. 904-13.
5. Hu X, De Silva TM, Chen J, and Faraci FM, *Cerebral Vascular Disease and Neurovascular Injury in Ischemic Stroke*. *Circ Res*, 2017. **120**(3): p. 449-71.
6. Krupinski J, Kaluza J, Kumar P, Kumar S, and Wang JM, *Role of angiogenesis in patients with cerebral ischemic stroke*. *Stroke*, 1994. **25**(9): p. 1794-8.
7. Arai K, Jin G, Navaratna D, and Lo EH, *Brain angiogenesis in developmental and pathological processes: neurovascular injury and angiogenic recovery after stroke*. *FEBS J*, 2009. **276**(17): p. 4644-52.
8. Kanazawa M, Takahashi T, Ishikawa M, Onodera O, Shimohata T, and Del Zoppo GJ, *Angiogenesis in the ischemic core: A potential treatment target?* *J Cereb Blood Flow Metab*, 2019. **39**(5): p. 753-69.
9. Ergul A, Alhusban A, and Fagan SC, *Angiogenesis: a harmonized target for recovery after stroke*. *Stroke*, 2012. **43**(8): p. 2270-4.
10. Hatakeyama M, Ninomiya I, and Kanazawa M, *Angiogenesis and neuronal remodeling after ischemic stroke*. *Neural Regen Res*, 2020. **15**(1): p. 16-19.
11. Darweesh RS, Ayoub NM, and Nazzal S, *Gold nanoparticles and angiogenesis: molecular mechanisms and biomedical applications*. *Int J Nanomedicine*, 2019. **14**: p. 7643-63.
12. Potente M, Gerhardt H, and Carmeliet P, *Basic and therapeutic aspects of angiogenesis*. *Cell*, 2011. **146**(6): p. 873-87.
13. Rust R, *Insights into the dual role of angiogenesis following stroke*. *J Cereb Blood Flow Metab*, 2020. **40**(6): p. 1167-71.
14. Sun P, Zhang K, Hassan SH, Zhang X, Tang X, Pu H, Stetler RA, Chen J, and Yin KJ, *Endothelium-Targeted Deletion of microRNA-15a/16-1 Promotes Poststroke Angiogenesis and Improves Long-Term Neurological Recovery*. *Circ Res*, 2020.

- 126**(8): p. 1040-57.
15. Deanfield JE, Halcox JP, and Rabelink TJ, *Endothelial function and dysfunction: testing and clinical relevance*. *Circulation*, 2007. **115**(10): p. 1285-95.
 16. Ferrara N, *Vascular endothelial growth factor: basic science and clinical progress*. *Endocr Rev*, 2004. **25**(4): p. 581-611.
 17. Miyake M, Goodison S, Urquidi V, Gomes Giacoia E, and Rosser CJ, *Expression of CXCL1 in human endothelial cells induces angiogenesis through the CXCR2 receptor and the ERK1/2 and EGF pathways*. *Lab Invest*, 2013. **93**(7): p. 768-78.
 18. Gertz K, Kronenberg G, Kalin RE, Baldinger T, Werner C, Balkaya M, Eom GD, Hellmann-Regen J, Krober J, Miller KR, Lindauer U, Laufs U, Dirnagl U, Heppner FL, and Endres M, *Essential role of interleukin-6 in post-stroke angiogenesis*. *Brain*, 2012. **135**(Pt 6): p. 1964-80.
 19. Brat DJ, Bellail AC, and Van Meir EG, *The role of interleukin-8 and its receptors in gliomagenesis and tumoral angiogenesis*. *Neuro Oncol*, 2005. **7**(2): p. 122-33.
 20. Hakanpaa L, Sipila T, Leppanen VM, Gautam P, Nurmi H, Jacquemet G, Eklund L, Ivaska J, Alitalo K, and Saharinen P, *Endothelial destabilization by angiopoietin-2 via integrin beta1 activation*. *Nat Commun*, 2015. **6**: p. 5962.
 21. Ferrara N and Adamis AP, *Ten years of anti-vascular endothelial growth factor therapy*. *Nat Rev Drug Discov*, 2016. **15**(6): p. 385-403.
 22. Apte RS, Chen DS, and Ferrara N, *VEGF in Signaling and Disease: Beyond Discovery and Development*. *Cell*, 2019. **176**(6): p. 1248-64.
 23. Wei MH, Popescu NC, Lerman MI, Merrill MJ, and Zimonjic DB, *Localization of the human vascular endothelial growth factor gene, VEGF, at chromosome 6p12*. *Hum Genet*, 1996. **97**(6): p. 794-7.
 24. Enomoto H, Inoki I, Komiya K, Shiomi T, Ikeda E, Obata K, Matsumoto H, Toyama Y, and Okada Y, *Vascular endothelial growth factor isoforms and their receptors are expressed in human osteoarthritic cartilage*. *Am J Pathol*, 2003. **162**(1): p. 171-81.
 25. Carmeliet P, Ferreira V, Breier G, Pollefeyt S, Kieckens L, Gertsenstein M, Fahrig M, Vandenhoeck A, Harpal K, Eberhardt C, Declercq C, Pawling J, Moons L, Collen D, Risau W, and Nagy A, *Abnormal blood vessel development and lethality in embryos lacking a single VEGF allele*. *Nature*, 1996. **380**(6573): p. 435-9.
 26. Gerber HP, Vu TH, Ryan AM, Kowalski J, Werb Z, and Ferrara N, *VEGF couples hypertrophic cartilage remodeling, ossification and angiogenesis during endochondral bone formation*. *Nat Med*, 1999. **5**(6): p. 623-8.
 27. Carlevaro MF, Cermelli S, Cancedda R, and Descalzi Cancedda F, *Vascular endothelial growth factor (VEGF) in cartilage neovascularization and chondrocyte differentiation: auto-paracrine role during endochondral bone formation*. *J Cell Sci*, 2000. **113** (Pt 1): p. 59-69.
 28. Greenberg DA and Jin K, *Vascular endothelial growth factors (VEGFs) and stroke*. *Cell Mol Life Sci*, 2013. **70**(10): p. 1753-61.
 29. Sun Y, Jin K, Xie L, Childs J, Mao XO, Logvinova A, and Greenberg DA, *VEGF-induced neuroprotection, neurogenesis, and angiogenesis after focal cerebral ischemia*. *J Clin Invest*, 2003. **111**(12): p. 1843-51.
 30. Harrigan MR, Ennis SR, Sullivan SE, and Keep RF, *Effects of intraventricular*

- infusion of vascular endothelial growth factor on cerebral blood flow, edema, and infarct volume. Acta Neurochir (Wien), 2003. 145(1): p. 49-53.*
31. Kaya D, Gursoy-Ozdemir Y, Yemisci M, Tuncer N, Aktan S, and Dalkara T, *VEGF protects brain against focal ischemia without increasing blood--brain permeability when administered intracerebroventricularly. J Cereb Blood Flow Metab, 2005. 25(9): p. 1111-8.*
 32. Ratcliffe PJ, *HIF-1 and HIF-2: working alone or together in hypoxia? J Clin Invest, 2007. 117(4): p. 862-5.*
 33. Ferrara N, Gerber HP, and LeCouter J, *The biology of VEGF and its receptors. Nat Med, 2003. 9(6): p. 669-76.*
 34. Zhang X, Gaspard JP, and Chung DC, *Regulation of vascular endothelial growth factor by the Wnt and K-ras pathways in colonic neoplasia. Cancer Res, 2001. 61(16): p. 6050-4.*
 35. Li J, Yen C, Liaw D, Podsypanina K, Bose S, Wang SI, Puc J, Miliareisis C, Rodgers L, McCombie R, Bigner SH, Giovanella BC, Ittmann M, Tycko B, Hibshoosh H, Wigler MH, and Parsons R, *PTEN, a putative protein tyrosine phosphatase gene mutated in human brain, breast, and prostate cancer. Science, 1997. 275(5308): p. 1943-7.*
 36. Giuliani N, Lunghi P, Morandi F, Colla S, Bonomini S, Hojden M, Rizzoli V, and Bonati A, *Downmodulation of ERK protein kinase activity inhibits VEGF secretion by human myeloma cells and myeloma-induced angiogenesis. Leukemia, 2004. 18(3): p. 628-35.*
 37. Lee CC, Chen SC, Tsai SC, Wang BW, Liu YC, Lee HM, and Shyu KG, *Hyperbaric oxygen induces VEGF expression through ERK, JNK and c-Jun/AP-1 activation in human umbilical vein endothelial cells. J Biomed Sci, 2006. 13(1): p. 143-56.*
 38. Dutra-Oliveira A, Monteiro RQ, and Mariano-Oliveira A, *Protease-activated receptor-2 (PAR2) mediates VEGF production through the ERK1/2 pathway in human glioblastoma cell lines. Biochem Biophys Res Commun, 2012. 421(2): p. 221-7.*
 39. Cheng RKY, Fiez-Vandal C, Schlenker O, Edman K, Aggeler B, Brown DG, Brown GA, Cooke RM, Dumelin CE, Dore AS, Geschwindner S, Grebner C, Hermansson NO, Jazayeri A, Johansson P, Leong L, Prihandoko R, Rappas M, Soutter H, Snijder A, Sundstrom L, Tehan B, Thornton P, Troast D, Wiggin G, Zhukov A, Marshall FH, and Dekker N, *Structural insight into allosteric modulation of protease-activated receptor 2. Nature, 2017. 545(7652): p. 112-15.*
 40. Vu TK, Hung DT, Wheaton VI, and Coughlin SR, *Molecular cloning of a functional thrombin receptor reveals a novel proteolytic mechanism of receptor activation. Cell, 1991. 64(6): p. 1057-68.*
 41. Yau MK, Lim J, Liu L, and Fairlie DP, *Protease activated receptor 2 (PAR2) modulators: a patent review (2010-2015). Expert Opin Ther Pat, 2016. 26(4): p. 471-83.*
 42. Mumaw MM, de la Fuente M, Noble DN, and Nieman MT, *Targeting the anionic region of human protease-activated receptor 4 inhibits platelet aggregation and thrombosis without interfering with hemostasis. J Thromb Haemost, 2014. 12(8): p. 1331-41.*

43. Dowal L, Sim DS, Dilks JR, Blair P, Beaudry S, Denker BM, Koukos G, Kuliopulos A, and Flaumenhaft R, *Identification of an antithrombotic allosteric modulator that acts through helix 8 of PAR1*. Proc Natl Acad Sci U S A, 2011. **108**(7): p. 2951-6.
44. Camerer E, Huang W, and Coughlin SR, *Tissue factor- and factor X-dependent activation of protease-activated receptor 2 by factor VIIa*. Proc Natl Acad Sci U S A, 2000. **97**(10): p. 5255-60.
45. Kahn ML, Hammes SR, Botka C, and Coughlin SR, *Gene and locus structure and chromosomal localization of the protease-activated receptor gene family*. J Biol Chem, 1998. **273**(36): p. 23290-6.
46. D'Andrea MR, Derian CK, Leturcq D, Baker SM, Brunmark A, Ling P, Darrow AL, Santulli RJ, Brass LF, and Andrade-Gordon P, *Characterization of protease-activated receptor-2 immunoreactivity in normal human tissues*. J Histochem Cytochem, 1998. **46**(2): p. 157-64.
47. Al-Ani B, Saifeddine M, Kawabata A, and Hollenberg MD, *Proteinase activated receptor 2: Role of extracellular loop 2 for ligand-mediated activation*. Br J Pharmacol, 1999. **128**(5): p. 1105-13.
48. Weis WI and Kobilka BK, *The Molecular Basis of G Protein-Coupled Receptor Activation*. Annu Rev Biochem, 2018. **87**: p. 897-919.
49. Suen JY, Adams MN, Lim J, Madala PK, Xu W, Cotterell AJ, He Y, Yau MK, Hooper JD, and Fairlie DP, *Mapping transmembrane residues of proteinase activated receptor 2 (PAR2) that influence ligand-modulated calcium signaling*. Pharmacol Res, 2017. **117**: p. 328-42.
50. Dulon S, Leduc D, Cottrell GS, D'Alayer J, Hansen KK, Bunnett NW, Hollenberg MD, Pidard D, and Chignard M, *Pseudomonas aeruginosa elastase disables proteinase-activated receptor 2 in respiratory epithelial cells*. Am J Respir Cell Mol Biol, 2005. **32**(5): p. 411-9.
51. Elmariah SB, Reddy VB, and Lerner EA, *Cathepsin S signals via PAR2 and generates a novel tethered ligand receptor agonist*. PLoS One, 2014. **9**(6): p. e99702.
52. Goh FG, Ng PY, Nilsson M, Kanke T, and Plevin R, *Dual effect of the novel peptide antagonist K-14585 on proteinase-activated receptor-2-mediated signalling*. Br J Pharmacol, 2009. **158**(7): p. 1695-704.
53. Hollenberg MD, Mihara K, Polley D, Suen JY, Han A, Fairlie DP, and Ramachandran R, *Biased signalling and proteinase-activated receptors (PARs): targeting inflammatory disease*. Br J Pharmacol, 2014. **171**(5): p. 1180-94.
54. Ramachandran R, Mihara K, Mathur M, Rochdi MD, Bouvier M, Defea K, and Hollenberg MD, *Agonist-biased signaling via proteinase activated receptor-2: differential activation of calcium and mitogen-activated protein kinase pathways*. Mol Pharmacol, 2009. **76**(4): p. 791-801.
55. Hilger D, Masureel M, and Kobilka BK, *Structure and dynamics of GPCR signaling complexes*. Nat Struct Mol Biol, 2018. **25**(1): p. 4-12.
56. Avet C, Sturino C, Grastilleur S, Gouill CL, Semache M, Gross F, Gendron L, Bennani Y, Mancini JA, Sayegh CE, and Bouvier M, *The PAR2 inhibitor I-287 selectively targets Galphaq and Galpha12/13 signaling and has anti-inflammatory effects*. Commun Biol, 2020. **3**(1): p. 719.

57. Stalheim L, Ding Y, Gullapalli A, Paing MM, Wolfe BL, Morris DR, and Trejo J, *Multiple independent functions of arrestins in the regulation of protease-activated receptor-2 signaling and trafficking*. Mol Pharmacol, 2005. **67**(1): p. 78-87.
58. Bucci M, Roviezzo F, and Cirino G, *Protease-activated receptor-2 (PAR2) in cardiovascular system*. Vascul Pharmacol, 2005. **43**(4): p. 247-53.
59. Noorbakhsh F, Vergnolle N, Hollenberg MD, and Power C, *Proteinase-activated receptors in the nervous system*. Nat Rev Neurosci, 2003. **4**(12): p. 981-90.
60. Johansson U, Lawson C, Dabare M, Syndercombe-Court D, Newland AC, Howells GL, and Macey MG, *Human peripheral blood monocytes express protease receptor-2 and respond to receptor activation by production of IL-6, IL-8, and IL-1{beta}*. J Leukoc Biol, 2005. **78**(4): p. 967-75.
61. Sekiguchi F, Takaoka K, and Kawabata A, *Proteinase-activated receptors in the gastrointestinal system: a functional linkage to prostanoids*. Inflammopharmacology, 2007. **15**(6): p. 246-51.
62. Hara T, Phuong PT, Fukuda D, Yamaguchi K, Murata C, Nishimoto S, Yagi S, Kusunose K, Yamada H, Soeki T, Wakatsuki T, Imoto I, Shimabukuro M, and Sata M, *Protease-Activated Receptor-2 Plays a Critical Role in Vascular Inflammation and Atherosclerosis in Apolipoprotein E-Deficient Mice*. Circulation, 2018. **138**(16): p. 1706-19.
63. Kagota S, Maruyama K, and McGuire JJ, *Characterization and Functions of Protease-Activated Receptor 2 in Obesity, Diabetes, and Metabolic Syndrome: A Systematic Review*. Biomed Res Int, 2016. **2016**: p. 3130496.
64. Crilly A, Palmer H, Nickdel MB, Dunning L, Lockhart JC, Plevin R, McInnes IB, and Ferrell WR, *Immunomodulatory role of proteinase-activated receptor-2*. Ann Rheum Dis, 2012. **71**(9): p. 1559-66.
65. Liu H, Liu F, Peng Y, Liu Y, Li L, Tu X, Cheng M, Xu X, Chen X, Ling G, and Sun L, *Role of mast cells, stem cell factor and protease-activated receptor-2 in tubulointerstitial lesions in IgA nephropathy*. Inflamm Res, 2010. **59**(7): p. 551-9.
66. Jin G, Hayashi T, Kawagoe J, Takizawa T, Nagata T, Nagano I, Syoji M, and Abe K, *Deficiency of PAR-2 gene increases acute focal ischemic brain injury*. J Cereb Blood Flow Metab, 2005. **25**(3): p. 302-13.
67. Morihara R, Yamashita T, Kono S, Shang J, Nakano Y, Sato K, Hishikawa N, Ohta Y, Heitmeier S, Perzborn E, and Abe K, *Reduction of intracerebral hemorrhage by rivaroxaban after tPA thrombolysis is associated with downregulation of PAR-1 and PAR-2*. J Neurosci Res, 2017. **95**(9): p. 1818-28.
68. Versteeg HH, Schaffner F, Kerver M, Ellies LG, Andrade-Gordon P, Mueller BM, and Ruf W, *Protease-activated receptor (PAR) 2, but not PAR1, signaling promotes the development of mammary adenocarcinoma in polyoma middle T mice*. Cancer Res, 2008. **68**(17): p. 7219-27.
69. Milia AF, Salis MB, Stacca T, Pinna A, Madeddu P, Trevisani M, Geppetti P, and Emanuelli C, *Protease-activated receptor-2 stimulates angiogenesis and accelerates hemodynamic recovery in a mouse model of hindlimb ischemia*. Circ Res, 2002. **91**(4): p. 346-52.
70. Cabral-Marques O, Marques A, Giil LM, De Vito R, Rademacher J, Gunther J, Lange

- T, Humrich JY, Klapa S, Schinke S, Schimke LF, Marschner G, Pitann S, Adler S, Dechend R, Muller DN, Braicu I, Sehouli J, Schulze-Forster K, Trippel T, Scheibenbogen C, Staff A, Mertens PR, Lobel M, Mastroianni J, Plattfaut C, Gieseler F, Dragun D, Engelhardt BE, Fernandez-Cabezudo MJ, Ochs HD, Al-Ramadi BK, Lamprecht P, Mueller A, Heidecke H, and Riemekasten G, *GPCR-specific autoantibody signatures are associated with physiological and pathological immune homeostasis*. Nat Commun, 2018. **9**(1): p. 5224.
71. Silosi I, Silosi CA, Boldeanu MV, Cojocaru M, Biciusca V, Avramescu CS, Cojocaru IM, Bogdan M, and FolcuTi RM, *The role of autoantibodies in health and disease*. Rom J Morphol Embryol, 2016. **57**(2 Suppl): p. 633-38.
 72. Ginsberg J and von Westarp C, *Clinical applications of assays for thyrotropin-receptor antibodies in Graves' disease*. CMAJ, 1986. **134**(10): p. 1141-7.
 73. Michalek K, Morshed SA, Latif R, and Davies TF, *TSH receptor autoantibodies*. Autoimmun Rev, 2009. **9**(2): p. 113-6.
 74. Reinsmoen NL, Lai CH, Heidecke H, Haas M, Cao K, Ong G, Naim M, Wang Q, Mirocha J, Kahwaji J, Vo AA, Jordan SC, and Dragun D, *Anti-angiotensin type I receptor antibodies associated with antibody mediated rejection in donor HLA antibody negative patients*. Transplantation, 2010. **90**(12): p. 1473-7.
 75. Cabral-Marques O and Riemekasten G, *Vascular hypothesis revisited: Role of stimulating antibodies against angiotensin and endothelin receptors in the pathogenesis of systemic sclerosis*. Autoimmun Rev, 2016. **15**(7): p. 690-4.
 76. Xia Y and Kellems RE, *Receptor-activating autoantibodies and disease: preeclampsia and beyond*. Expert Rev Clin Immunol, 2011. **7**(5): p. 659-74.
 77. Chen L, *Funktionelle Charakterisierung der endothelvermittelten autoimmunen PAR-2 Aktivierung in Charité-Universitätsmedizin Berlin*. 2020, (Accessed 2020-06-17T08:41:41Z, at <https://refubium.fu-berlin.de/handle/fub188/27311>).
 78. Li Q, *Autoimmune PAR2 activation in vascular events*, in Charité-Universitätsmedizin Berlin. 2021, (Accessed 2021-09-15T11:26:20Z, at <https://refubium.fu-berlin.de/handle/fub188/30548>).
 79. Carpentier G, Berndt S, Ferratge S, Rasband W, Cuendet M, Uzan G, and Albanese P, *Angiogenesis Analyzer for ImageJ - A comparative morphometric analysis of "Endothelial Tube Formation Assay" and "Fibrin Bead Assay"*. Sci Rep, 2020. **10**(1): p. 11568.
 80. Finkenzeller G, Sparacio A, Technau A, Marme D, and Siemeister G, *Sp1 recognition sites in the proximal promoter of the human vascular endothelial growth factor gene are essential for platelet-derived growth factor-induced gene expression*. Oncogene, 1997. **15**(6): p. 669-76.
 81. Cheng Z, Garvin D, Paguio A, Stecha P, Wood K, and Fan F, *Luciferase Reporter Assay System for Deciphering GPCR Pathways*. Curr Chem Genomics, 2010. **4**: p. 84-91.
 82. Bang E, Kim DH, and Chung HY, *Protease-activated receptor 2 induces ROS-mediated inflammation through Akt-mediated NF-kappaB and FoxO6 modulation during skin photoaging*. Redox Biol, 2021. **44**: p. 102022.
 83. Calebiro D and Godbole A, *Internalization of G-protein-coupled receptors:*

- Implication in receptor function, physiology and diseases.* Best Pract Res Clin Endocrinol Metab, 2018. **32**(2): p. 83-91.
84. January B, Seibold A, Allal C, Whaley BS, Knoll BJ, Moore RH, Dickey BF, Barber R, and Clark RB, *Salmeterol-induced desensitization, internalization and phosphorylation of the human beta2-adrenoceptor.* Br J Pharmacol, 1998. **123**(4): p. 701-11.
 85. Dong W, Li Y, Gao M, Hu M, Li X, Mai S, Guo N, Yuan S, and Song L, *IKKalpha contributes to UVB-induced VEGF expression by regulating AP-1 transactivation.* Nucleic Acids Res, 2012. **40**(7): p. 2940-55.
 86. Ehlers M, Allelein S, and Schott M, *TSH-receptor autoantibodies: pathophysiology, assay methods, and clinical applications.* Minerva Endocrinol, 2018. **43**(3): p. 323-32.
 87. Morshed SA and Davies TF, *Graves' Disease Mechanisms: The Role of Stimulating, Blocking, and Cleavage Region TSH Receptor Antibodies.* Horm Metab Res, 2015. **47**(10): p. 727-34.
 88. Schur PH, *IgG subclasses. A historical perspective.* Monogr Allergy, 1988. **23**: p. 1-11.
 89. Koneczny I, *A New Classification System for IgG4 Autoantibodies.* Front Immunol, 2018. **9**: p. 97.
 90. Zuo Y, Evangelista F, Culton D, Guilbert A, Lin L, Li N, Diaz L, and Liu Z, *IgG4 autoantibodies are inhibitory in the autoimmune disease bullous pemphigoid.* J Autoimmun, 2016. **73**: p. 111-9.
 91. Cojocaru IM, Cojocaru M, and Burcin C, *IgG-autoantibodies against oxidized low-density lipoprotein in ischemic stroke onset.* Rom J Intern Med, 2006. **44**(2): p. 165-70.
 92. Ayoub MA and Pin JP, *Interaction of Protease-Activated Receptor 2 with G Proteins and beta-Arrestin 1 Studied by Bioluminescence Resonance Energy Transfer.* Front Endocrinol (Lausanne), 2013. **4**: p. 196.
 93. McCoy KL, Traynelis SF, and Hepler JR, *PAR1 and PAR2 couple to overlapping and distinct sets of G proteins and linked signaling pathways to differentially regulate cell physiology.* Mol Pharmacol, 2010. **77**(6): p. 1005-15.
 94. Zhao J, Deng Y, Jiang Z, and Qing H, *G Protein-Coupled Receptors (GPCRs) in Alzheimer's Disease: A Focus on BACE1 Related GPCRs.* Front Aging Neurosci, 2016. **8**: p. 58.
 95. New DC and Wong YH, *Molecular mechanisms mediating the G protein-coupled receptor regulation of cell cycle progression.* J Mol Signal, 2007. **2**: p. 2.
 96. DeFea KA, Zalevsky J, Thoma MS, Dery O, Mullins RD, and Bunnett NW, *beta-arrestin-dependent endocytosis of proteinase-activated receptor 2 is required for intracellular targeting of activated ERK1/2.* J Cell Biol, 2000. **148**(6): p. 1267-81.
 97. Ge L, Ly Y, Hollenberg M, and DeFea K, *A beta-arrestin-dependent scaffold is associated with prolonged MAPK activation in pseudopodia during protease-activated receptor-2-induced chemotaxis.* J Biol Chem, 2003. **278**(36): p. 34418-26.
 98. Joyal JS, Nim S, Zhu T, Sitaras N, Rivera JC, Shao Z, Sapieha P, Hamel D, Sanchez

- M, Zaniolo K, St-Louis M, Ouellette J, Montoya-Zavala M, Zabeida A, Picard E, Hardy P, Bhosle V, Varma DR, Gobeil F, Jr., Beausejour C, Boileau C, Klein W, Hollenberg M, Ribeiro-da-Silva A, Andelfinger G, and Chemtob S, *Subcellular localization of coagulation factor II receptor-like 1 in neurons governs angiogenesis*. Nat Med, 2014. **20**(10): p. 1165-73.
99. Chang LH, Pan SL, Lai CY, Tsai AC, and Teng CM, *Activated PAR-2 regulates pancreatic cancer progression through ILK/HIF-alpha-induced TGF-alpha expression and MEK/VEGF-A-mediated angiogenesis*. Am J Pathol, 2013. **183**(2): p. 566-75.
 100. Rasmussen JG, Riis SE, Frobert O, Yang S, Kastrup J, Zachar V, Simonsen U, and Fink T, *Activation of protease-activated receptor 2 induces VEGF independently of HIF-1*. PLoS One, 2012. **7**(9): p. e46087.
 101. Catar R, Witowski J, Zhu N, Lucht C, Derrac Soria A, Uceda Fernandez J, Chen L, Jones SA, Fielding CA, Rudolf A, Topley N, Dragun D, and Jorres A, *IL-6 Trans-Signaling Links Inflammation with Angiogenesis in the Peritoneal Membrane*. J Am Soc Nephrol, 2017. **28**(4): p. 1188-99.
 102. Schaider H, Oka M, Bogenrieder T, Nesbit M, Satyamoorthy K, Berking C, Matsushima K, and Herlyn M, *Differential response of primary and metastatic melanomas to neutrophils attracted by IL-8*. Int J Cancer, 2003. **103**(3): p. 335-43.
 103. Wei ZW, Xia GK, Wu Y, Chen W, Xiang Z, Schwarz RE, Brekken RA, Awasthi N, He YL, and Zhang CH, *CXCL1 promotes tumor growth through VEGF pathway activation and is associated with inferior survival in gastric cancer*. Cancer Lett, 2015. **359**(2): p. 335-43.
 104. Veikkola T and Alitalo K, *Dual role of Ang2 in postnatal angiogenesis and lymphangiogenesis*. Dev Cell, 2002. **3**(3): p. 302-4.
 105. Maisonpierre PC, Suri C, Jones PF, Bartunkova S, Wiegand SJ, Radziejewski C, Compton D, McClain J, Aldrich TH, Papadopoulos N, Daly TJ, Davis S, Sato TN, and Yancopoulos GD, *Angiopoietin-2, a natural antagonist for Tie2 that disrupts in vivo angiogenesis*. Science, 1997. **277**(5322): p. 55-60.
 106. Holash J, Wiegand SJ, and Yancopoulos GD, *New model of tumor angiogenesis: dynamic balance between vessel regression and growth mediated by angiopoietins and VEGF*. Oncogene, 1999. **18**(38): p. 5356-62.
 107. Harterich S, Koschatzky S, Einsiedel J, and Gmeiner P, *Novel insights into GPCR-peptide interactions: mutations in extracellular loop 1, ligand backbone methylations and molecular modeling of neurotensin receptor 1*. Bioorg Med Chem, 2008. **16**(20): p. 9359-68.
 108. Murphy JW and Kendall DA, *Integrity of extracellular loop 1 of the human cannabinoid receptor 1 is critical for high-affinity binding of the ligand CP 55,940 but not SR 141716A*. Biochem Pharmacol, 2003. **65**(10): p. 1623-31.
 109. Zhu N, *Development of a molecular toolbox to study the cross-talk between Angiotensin II type 1 and Endothelin-1 type A receptors in the context of obliterative vasculopathy*, in Charité-Universitätsmedizin Berlin. 2015, (Accessed 2015-12-07T12:11:19.838Z, at <https://refubium.fu-berlin.de/handle/fub188/2530>).
 110. Banerjee AA and Mahale SD, *Extracellular loop 3 substitutions K589N and A590S in*

FSH receptor increase FSH-induced receptor internalization and along with S588T substitution exhibit impaired ERK1/2 phosphorylation. Arch Biochem Biophys, 2018. **659**: p. 57-65.

111. Lynagh T, Khamu TS, and Bryan-Lluka LJ, *Extracellular loop 3 of the noradrenaline transporter contributes to substrate and inhibitor selectivity.* Naunyn Schmiedebergs Arch Pharmacol, 2014. **387**(1): p. 95-107.

Statutory Declaration

“I, Hongfan Zhao, by personally signing this document in lieu of an oath, hereby affirm that I prepared the submitted dissertation on the topic Stroke dependent mechanisms of endothelial autoimmune PAR2 activation/Schlaganfall abhängige Mechanismen der endothelialen autoimmunnen PAR2 Aktivierung, independently and without the support of third parties, and that I used no other sources and aids than those stated.

All parts which are based on the publications or presentations of other authors, either in letter or in spirit, are specified as such in accordance with the citing guidelines. The sections on methodology (in particular regarding practical work, laboratory regulations, statistical processing) and results (in particular regarding figures, charts and tables) are exclusively my responsibility.

Furthermore, I declare that I have correctly marked all of the data, the analyses, and the conclusions generated from data obtained in collaboration with other persons, and that I have correctly marked my own contribution and the contributions of other persons (All blood samples were collected from collaborative group, PD. Dr. Thomas G Liman). I have correctly marked all texts or parts of texts that were generated in collaboration with other persons.

My contributions to any publications to this dissertation correspond to those stated in the below joint declaration made together with the supervisor. All publications created within the scope of the dissertation comply with the guidelines of the ICMJE (International Committee of Medical Journal Editors; www.icmje.org) on authorship. In addition, I declare that I shall comply with the regulations of Charité – Universitätsmedizin Berlin on ensuring good scientific practice.

I declare that I have not yet submitted this dissertation in identical or similar form to another Faculty.

The significance of this statutory declaration and the consequences of a false statutory declaration under criminal law (Sections 156, 161 of the German Criminal Code) are known to me.”

Date

Signature

Curriculum Vitae

My curriculum vitae does not appear in the electronic version of my paper for reasons of data protection.

Publications

Publication 1: Catar R, Chen L, **Zhao H**, Wu D, Julian Kamhieh-Milz, Lücht C, Zickler D, W. Krug A, G. Ziegler C, Morawietz H, Witowski J. Native and Oxidized Low-Density Lipoproteins Increase the Expression of the LDL Receptor and the LOX-1 Receptor, Respectively, in Arterial Endothelial Cells. *Cells* 2022, 11(2), 204; <https://doi.org/10.3390/cells11020204>

Publication 2: Simon M, Lücht C, Hosp I, **Zhao H**, Wu D, Heidecke H, Witowski J, Budde K, Riemekasten G, Catar R. Autoantibodies from Patients with Scleroderma Renal Crisis Promote PAR-1 Receptor Activation and IL-6 Production in Endothelial Cells. *Int J Mol Sci.* 2021 Oct 30; 22 (21):11793. doi: 10.3390/ijms222111793.

Publication 3: Catar R, Moll G, Hosp I, Simon M, Luecht C, **Zhao H**, Wu D, Chen L, Kamhieh-Milz J, Korybalska K, Zickler D, Witowski J. Transcriptional Regulation of Thrombin-Induced Endothelial VEGF Induction and Proangiogenic Response. *Cells.* 2021 Apr 15; 10 (4):910. doi: 10.3390/cells10040910.

Publication 4: Catar R, Moll G, Kamhieh-Milz J, Luecht C, Chen L, **Zhao H**, Ernst L, Willy K, Girndt M, Fiedler R, Witowski J, Morawietz H, Ringdén O, Dragun D, Eckardt KU, Schindler R, Zickler D. Expanded Hemodialysis Therapy Ameliorates Uremia-Induced Systemic Microinflammation and Endothelial Dysfunction by Modulating VEGF, TNF- α and AP-1 Signaling. *Front Immunol.* 2021 Nov 11; 12:774052. doi: 10.3389/fimmu.2021.774052. eCollection 2021.

Publication 5: Catar RA, Chen L, Cuff SM, Kift-Morgan A, Eberl M, Kettritz R, Kamhieh-Milz J, Moll G, Li Q, **Zhao H**, Kawka E, Zickler D, Parekh G, Davis P, Fraser DJ, Dragun D, Eckardt KU, Jörres A, Witowski J. Control of neutrophil influx during peritonitis by transcriptional cross-regulation of chemokine CXCL1 by IL-17 and IFN- γ . *J Pathol.* 2020 Jun; 251(2):175-186. doi:10.1002/path.5438. Epub 2020 May.

Acknowledgements

In the beginning, I would like to thank my supervisors, Prof. Dr. Duska Dragun and Prof. Dr. Klemens Budde, who gave me the chance to study in Charite and offered me the wonderful platform where I can work with excellent scientific researchers and finish my doctoral thesis. It has been a great time studying here during three years.

Apart from my supervisor, I would like to express sincere gratitude to my junior supervisor Dr. Rusan Catar for giving me many pertinent suggestions and continuous support for my doctoral research work. Thank you for introducing doctoral project to me, and showing me all experiment items and methods patiently. Without his patient guidance on my experiments and thesis writing, this work can not be finished in time. It will be really hard for me to forget his guidance throughout my life!

Next, I would say thanks to the professional scientists Aurelie Philippe, and Angelika Kusch for the valuable suggestions for my doctoral thesis and relevant research work. Thank you, Marc, for the help in methods, techniques and general issues. Thank you, my colleagues, Chen Lei, Ren Peng, Qing Li, Dashan Wu, Michael Adu Gyamfi for the companionship, help and the fun-time we spent together.

In the end, I would like to thank my family, Dan Wang, my parents and parents-in-law. Thank you for permanent support and understanding, both for my career, and my personal life. Encouragement, motivation and financial support from you give me the power to achieve my objective along the way. Thank you so much!

In the past 3 years, too much help and support from my colleagues, family and relatives motivated me to finish my doctoral thesis. I sincerely wish them health and happiness every day. Thank you!

Confirmation by a statistician



CharitéCentrum für Human- und Gesundheitswissenschaften

Charité | Campus Charité Mitte | 10117 Berlin

Institut für Biometrie und klinische Epidemiologie (iBike)

Direktor: Prof. Dr. Geraldine Rauch

Name, Vorname: Zhao, Hongfan

Emailadresse: hongfan.zhao@charite.de

Matrikelnummer: 226594

PromotionsbetreuerIn: Klemens Budde

Promotionsinstitution / Klinik: Charité Berlin / Klinik für Nephrologie und Intensivmedizin

Postanschrift:
Charitéplatz 1 | 10117 Berlin
Besucheranschrift:
Reinhardtstr. 58 | 10117 Berlin

Tel. +49 (0)30 450 562171
geraldine.rauch@charite.de
<https://biometrie.charite.de/>



Bescheinigung

Hiermit bescheinige ich, dass Herrn *Hongfan Zhao* innerhalb der Service Unit Biometrie des Instituts für Biometrie und klinische Epidemiologie (iBike) bei mir eine statistische Beratung zu einem Promotionsvorhaben wahrgenommen hat. Folgende Beratungstermine wurden wahrgenommen:

- Termin 1: 17.01.2022

Folgende wesentliche Ratschläge hinsichtlich einer sinnvollen Auswertung und Interpretation der Daten wurden während der Beratung erteilt:

- Allgemeine Hinweise zum Aufbau und Struktur der Monographie
- Überarbeitung der Grafiken empfohlen
- Problematik der α -Fehler-Kumulierung bei multiplen Testen erörtert

Diese Bescheinigung garantiert nicht die richtige Umsetzung der in der Beratung gemachten Vorschläge, die korrekte Durchführung der empfohlenen statistischen Verfahren und die richtige Darstellung und Interpretation der Ergebnisse. Die Verantwortung hierfür obliegt allein dem Promovierenden. Das Institut für Biometrie und klinische Epidemiologie übernimmt hierfür keine Haftung.

Datum: 17.01.2022

Name des Beraters: Lukas Mödl

Lukas Moedl

Digital unterschrieben von Lukas Moedl
Datum: 2022.01.27 00:10:24 +01'00'

Unterschrift BeraterIn, Institutsstempel

